University Of Jordan

Faculty Of Graduate Studies

UTILIZATION OF VIBRATION MODE SHAPES FOR CRACK IDENTIFICATION OF CANTILEVER BEAMS

BY

NIDAL A. F. ABU AL-RUB

SUPERVISOR

Dr. M. H. DADO

CO-SUPERVISOR

Dr. A. TAYEM

Submitted in partial fulfillment of the requirements for the degree

of Master of Science in Mechanical Engineering.

Faculty of Graduate Studies,

University of Jordan

Amman Jordan

April, 1993

This thesis was defended successfully on 28th, April, 1993.

COMMITTEE MEMBERS	SIGNATURE
1. Dr. Mohammad h. Dado	
2. Dr. Adel A. Tayem	
3. Dr. Mazen Al-Qaisi	
4. Dr. Mohammed N. Hamdan	
5. Dr. Saad Al-Habali	

To whom I owe my life
to my parents with love and appreciation

ACKNOWLEDGEMENTS

It is with deep pleasure I express my gratitude to all who helped me during the preparation and completion of this work. Special thanks are indebted to my supervisor, Dr. Mohammed H. Dado, and Dr. Adel A. Tayem whom without their support, encouragement, and advice, my work could have been more difficult. Also I express my thanks to Dr. Mohammed N. Hamdan for his help.

Finally, I should not forget the support given to me by my uncle As'ad Abu Al-Rub and by all my friends throughout my study.

Contents

List of Tables

List of Figures

NOMENCLATURE

c	is the compliance;
E	is the modules of elasticity of the beam material $\frac{N}{m^2}$;
I	is the moment of inertia m^4;
$I(\frac{a}{h})$	dimentionless local compliance function;
a	is the depth of the crack;
h	is the depth of the specimens;
L_1	the distance from the crack position to the clamped end;
L	total length of the beam;
w	is the natural frequency $(\frac{rad.}{s})$;
K	spring constant at the clamped end $(\frac{N.m}{rad.})$;
K_T	spring constant at the crack location $(\frac{N.m}{rad.})$;
A_i	are constants, i=1,2;
B_i	are constants, i=1,2;
C_i	are constants, i=1,2;
D_i	are constants, i=1,2;
V_n	normalized voltage which equal to $\frac{V-V_c}{V_t-V_c}$;
V_t	the voltage at the tip of the specimens in mv;
V_c	the voltage at the clamped end of the specimens in mv;
V	the voltage at any location on the specimens in mv;

GreekSymbols

ρ	the mass of the beam per unit length $\frac{k_2}{m}$;
β_i	are constants, i=1,..., 4;
ψ_i	are constants, i=1,...., 12;
η_i	are constants, i=1,...., 8;
λ	is constant, where $\lambda^4 = \frac{\rho\omega^2}{EI}$;

ABSTRACT

The main topic of this study is to examine theoretically and experimentally the dynamic behaviour of cracked cantilever beams. The effect of the crack over the natural frequency of the first mode was the bases of this examination. The outcome of this detailed examination helps in discovering and detecting the crack parameters, both: the location and the depth.

In this study, one of the old ways of detecting cracks was re-examined. Few faults were discovered in that method . A new method for crack detection which is thought to be more effective and comprehensive is proposed to replace that old one. Computer programs were developed in order to solve the equations that have been derived in this study. The solution of these equations delivered the theoretical parameters necessary for crack identification. Finally, several conclusions and recommendations are discussed to open new areas in utilizing vibration techniques in crack detection.

Chapter 1

INTRODUCTION

The increased demand on improving quality and methods of maintenance has led researchers to look for new and inexpensive methods in testing specimens. No doubt, that using the vibration techniques is cheaper and easier than the Radiographic and Ultrasonic methods. In addition , the vibration techniques are non-destructive techniques.

Beams that are made of Mild Steel are used enormously in constructions. It would be useful if we could study these beams specially the cantilever beams. This study will focus attention on cantilever beams and the effect of damage over dynamic response for beams that have cracks or slots. Cracks have an effect on beam compliance. Accordingly, this leads to an influence on mode shapes of the specimens specially on the first mode. This phenomenon was employed in this study to detect cracks (its location and depth).

In this research a bending spring is used to model the crack. Also a bending spring is used as a representation of the partially restraint end. Therefore, the dynamic behaviour parameters (for example; natural frequency, amplitudes, ... etc) for the specimens could be evaluated theoretically.

The method of vibration to detect cracks is a new one, and still needs more research work, specially to make sure that conclusions of these research are reliable.

This method is employed in this study in order to get a systematic procedure that could be followed in testing cracked cantilevers. This study might be a contribution in a comprehensive technique in testing frame structures in the future.

In 1990 a new method was suggested to detect cracks, but it was not adequately-effective. In the present work few faults were discovered in that method. So a new method is proposed to replace it. Previous studies are covered in the next Chapter

.

1.1 Thesis Layout

Following this chapter, a literature Review is presented in Chapter II. Chapter III contains the theoretical derivation of the equation of motion. The experimental set-up and data collection are presented in Chapter IV. Chapter V include the results and discussions. The conclusions and recommendations are stated in Chapter VI.

Chapter 2

LITERATURE REVIEW

The problem of crack identification and the crack effect over the dynamic response has been studied by many investigators. Chondros and Dimarogonas [1], modeled the crack as a local flexibility determined using fracture mechanics methods. They measured it experimentally and developed spectral method to identify cracks in various structures. They related the crack depth to the change in natural frequencies of the first three harmonics of the structure for known crack position. Dimarogonas [2], and Dimarogonas and Paipetis [3] calculated the bending spring constant k_T in the cracked section of a beam with orthogonal cross-section of width b and high h as shown in Figure 2.1. The spring constant K_T is calculated for a lateral crack of uniform depth, using the crack strain energy function. They found that [1]

$$K_T = \frac{1}{c} \tag{2.1}$$

$$c = (5.346h/EI)I(a/h)$$

Where c is the compliance, E is the modules of elasticity of the beam material, I is the moment of inertia of the beam cross-section. The dimensionless local compliance function $I(a/h)$ is computed from the strain energy density function and has the

[1] from Rizos et al. [13]

form.

$$I(a/h) = 1.8624(a/h)^2 - 3.95(a/h)^3 + 16.375(a/h)^4 - 37.226(a/h)^5$$

$$+76.81(a/h)^6 - 126.9(a/h)^7 + 172(a/h)^8 - 143.97(a/h)^9$$

$$+66.56(a/h)^{10}$$

Anifantis et al. [4] further developed the spectral method for identification the earth-quake induced defects in reinforced concrete frames by analysis of the changes in the vibration frequency spectral. They also showed that any localized damage, such as a crack, would affect each vibration mode differently for various structures depending on particular location, orientation, and magnitude of the crack. Kirshmer [5], Thomson [6], and Petroski [7,8] illustrated the effects of cracks on structural response through simple reduced section models of cracked beams using energy methods. They discussed the effect of size and location of the crack on the natural frequency and vibration mode of the damaged beam. Grabowski [9] came to the conclusion that there is a strong dependence of vibration behavior of cracked rotors on the crack position and magnitude.

Inagaki et al. [10] estimated the crack size and position by natural vibration analysis and by static deflection analysis in the case of transverse vibrations of cracked rotor.

Christides and Barr [11] derived the equation of bending motion for a Bernoulli-Euler beam containing pairs of symmetric open cracks. The cracks were taken to be normal to the beams neutral axis and symmetrical about the plane of bending

as shown in Figure 2.2. They used an exponential-type function to model the stress concentration near the crack tip. The rate of stress decay from the crack was controlled by a dimensionless parameter α that was determined by fitting the analytical results with experimental data. The assumptions of Christides and Barr for cracked beam in bending are those of Bernoulli- Euller theory, except that the normal stress and strain are modified to account for the stress concentration near the crack tip.

Rajab and Al-Sabeeh [12] analytically derived expressions and presented plots relating the crack depth and location of cracked Timoshinko shaft in the first few natural frequencies of the shaft as shown in Figure 2.3, these expressions were obtained by modeling the crack as bending and shear compliances of equivalent incremental strain energy by using the J-integral concept from fracture mechanics. It is shown that knowledge of the changes in the first three natural frequencies relative to estimate the crack depth and crack location in the shaft.

Rizos et al. [13] related the measured vibration amplitude to the cracks location and depth, they used analytical and experimental results of flexural vibration of a beam with rectangular cross-section having a transverse surface crack extending uniformly along the width of the beam. The crack was represented by bending spring. The value of this spring was estimated by utilizing eq.(2.1), which is mentioned above. They mentioned that, from the measured amplitudes at two points of the structure vibrating at one of its natural modes, the crack location and its magnitude can be estimated with satisfactory accuracy. Table (2.1) shows their results, while Figure 2.4 shows the measured first three mode shapes for cracked beam has a crack at 140mm position from the clamped end and at a depth of 10mm. A 300mm cantilever beam of cross-section 20mmx20mm was used in that study. Figure 2.5

shows the measurement system used in that study.

Caweley [14] reports a series of tests on a cantilever beam with slots of different depths located at 1 millimeter from the root. The beam was 250 mm long, 15 mm wide, and 10 mm deep. The slots were introducing a 1.6 mm diameter cutter. These slots have uniform depth across the cross section of the beam. The changes produced by these slots of different depths in the natural frequencies for the first four modes of flexible axis of the beam were measured. Subsequently, attempts were made to predict the size of the natural frequency changes using finite element analysis. The element used was two dimensional, and the analysis was carried out using the FINEL package developed at Imperial college. The defect was modelled by unpinning nodes at the root of the beam. The results of this analysis for modes 1 and 4 are shown as solid lines in Figure 2.6, where the solid line represent the measured results. It is clear that the predicted changes due the cracks are significantly smaller than those measured for slots.

Caweley et al. [15] have studied the effect of slot width on the natural frequency changes produced by the introduction of slots in beams they found that the natural frequency changes do increase with increasing slot width. However, their results were for slots which where much wider than the cracks , this was done by testing specimens with slots of the profiles shown in Figure 2.7, all of which had a width of 1.6 mm. It was found that the natural frequency changes produced by slots of different profiles correlated well with the reduction in the second moment of area of the cross section of the bar at the defect location about the center of area of the section. This is demonstrated in Figure 2.8, which shows the natural frequency change in the third mode as a function of the change in second moment of the cross

section at the defect location for all the sets carried out with slots 1.6 mm wide.

Ismail et al. [16] mentioned that vibration measurements can offer an effective, inexpensive, and fast means of nondestructive testing of structures. their work investigated of the effect of crack closure on the frequency changes of cracked cantilever beams. The study has been conducted by using both computer simulations and experimental modal analysis.

2.1 Significance of The Study

Taking the previous research in consideration, the use of vibration methods in detecting cracks is new. However, it still needs more research and studies to increase its reliability. Particularly, the effect of crack on the fundamental mode and on the dynamic behavior of the beam. This study will examine these issues theoretically and experimentally. Anew procedure is described for crack identification as a new contribution in this area.

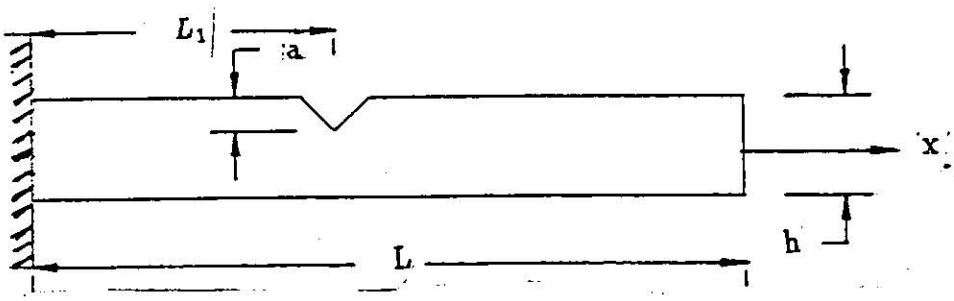

Figure 2.1: cracked beam

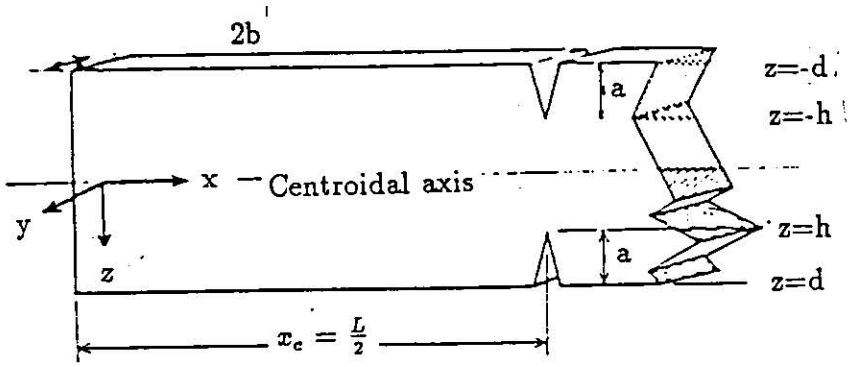

Figure 2.2: Beam has two symmetric open crack [11]

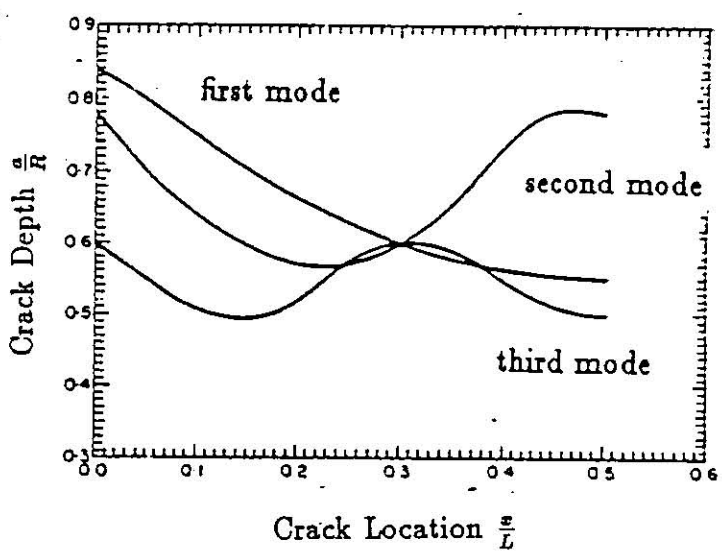

Figure 2.3: The crack depth Vs. crack location for the shaft[12]

Measured		Calculated	Error		Calculated	Error	
Position	Depth	position	%	r.m.s	depth	%	r.m.s.
10	2	10·31	3·00	3·937	2·08	4·00	4·645
	6	9·92	−1·00		5·89	−1·83	
	10	10·41	4·00		10·40	4·00	
	14	10·62	6·00		14·72	7·14	
80	2	78·61	1·75	5·561	1·95	−2·50	4·448
	6	80·93	1·12		6·32	5·33	
	10	83·31	4·12		9·82	−1·80	
	14	71·91	−10·12		14·90	6·42	
140	2	138·72	−0·92	3·132	1·91	−4·50	4·602
	6	139·41	−0·42		6·38	6·33	
	10	145·51	3·92		9·71	−2·90	
	14	146·71	4·78		13·44	−4·00	
200	2	200·72	0·35	3·664	2·10	5·00	4·991
	6	200·13	0·05		5·60	−6·66	
	10	210·43	5·20		9·45	5·50	
	14	189·72	−5·15		13·95	−0·36	
260	2	275·81	6·07	7·605	2·13	6·50	7·970
	6	235·22	−9·54		5·38	−2·83	
	10	278·22	7·00		9·31	−6·90	
	14	240·81	−7·38		15·75	12·50	

Table 2.1: Comparison of actual and estimated crack position and depth (all dimension in mm)[13]

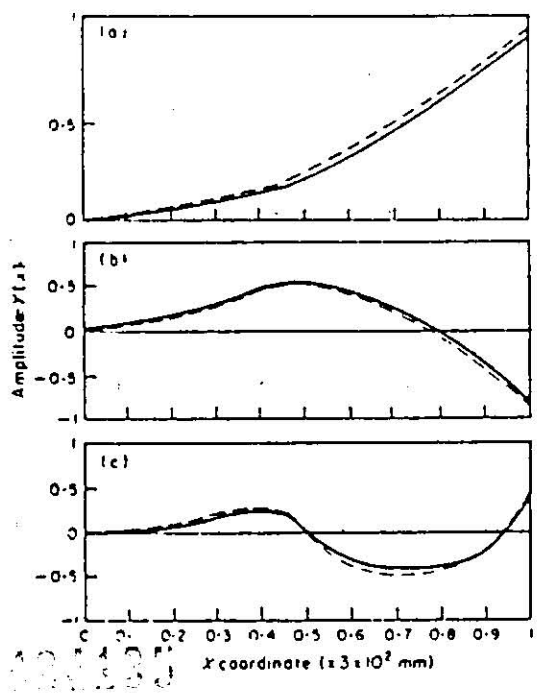

Figure 2.4: Comparison of measured (- - -) and calculated (—) results for the lowest three vibration modes. (a) First mode. 171 Hz. (b) second mode. 987 Hz. (c)third mode. 3034 Hz [13]

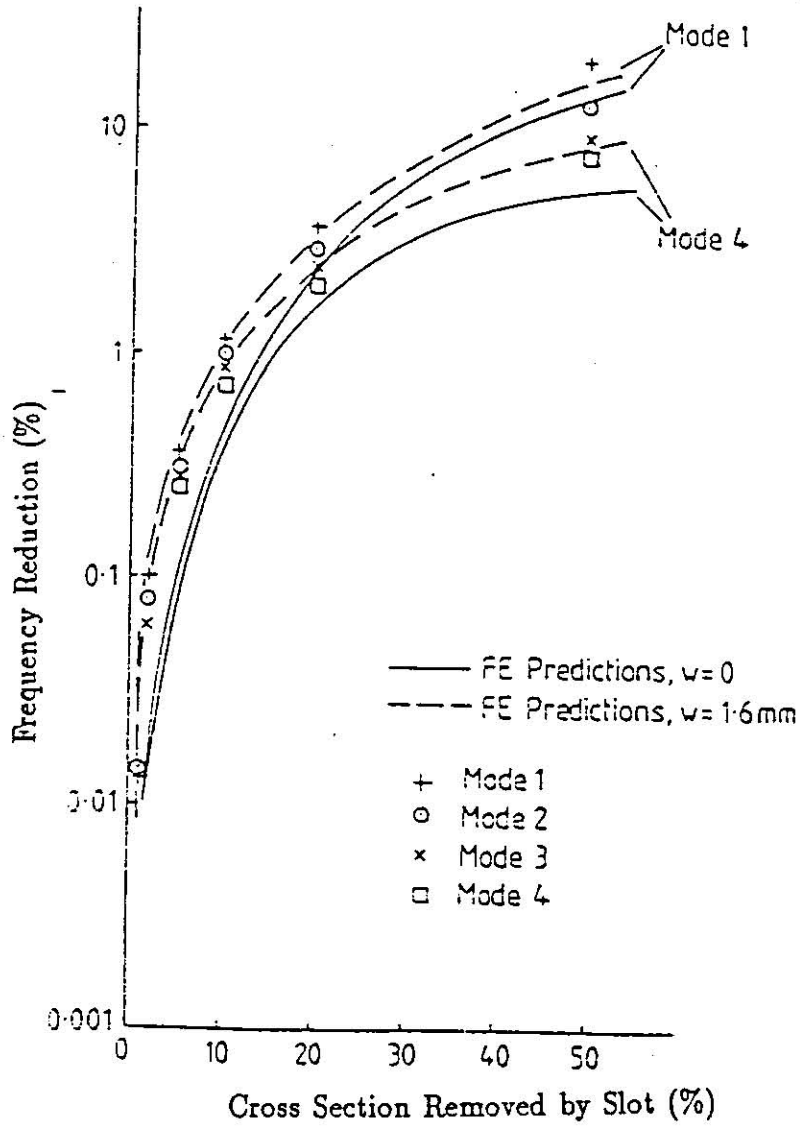

Figure 2.6: Experimentally measured natural frequency changes due to slots 1.6mm wide, 1mm from the root of a cantilever beam, together with finite element predictions obtained by unpinning nodes at the root of the beam(w=0) and by modeling the defect as a slot 1.6mm wide (w=1.6mm) [14]

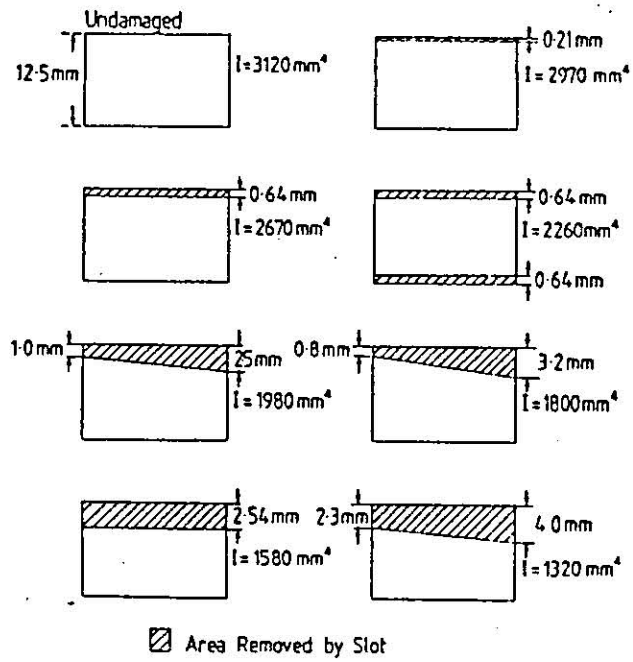

Figure 2.7: Slot profiles tested.(I=second moment of area of section about an axis through the center of area of the section, parallel to the base of the section.)[15]

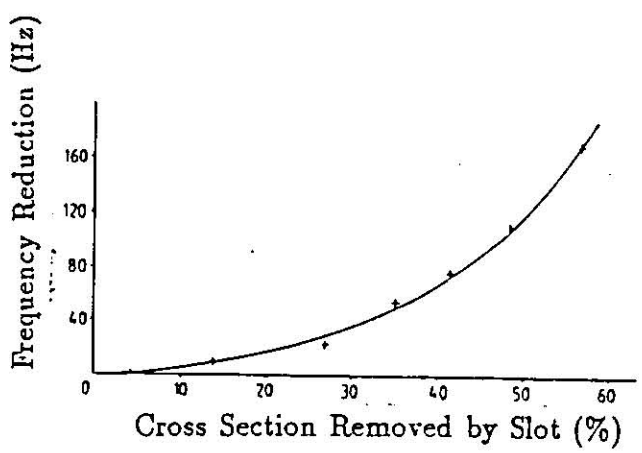

Figure 2.8: Variation in third mode natural frequency with second moment of area of damaged section for beams with slot profiles shown in the previous Figure[15]

Chapter 3

THEORY and MATHEMATICAL MODELING

In this chapter, the theoretical derivation for the cantilever beam using Euler equation will be discussed. A set of assumptions is developed to make the theoretical study feasible. In the following, the governing equations are derived using some simplifying assumptions.

3.1 The Basic Equation and The Simplifying Assumptions

The basic equation that governs the motion of an elastic beam is given by Euler equation which states that

$$EI\frac{d^4y}{dx^4} - \rho w^2 y = 0 \tag{3.1}$$

Where

ρ= mass of beam per unit length $(\frac{Kg}{m})$

ω= natural frequency $(\frac{rad.}{s})$

E= modules of elasticity $(\frac{N}{m^2})$

I= area moment of inertia (m^4)

By making

$$\lambda^4 = \frac{\rho w^2}{EI}$$

One obtains the following forth order differential equation:

$$\frac{d^4y}{dx^4} - \lambda^4 y = 0 \tag{3.2}$$

For the vibration of a uniform beam. The general solution for this equation is:

$$y = Acos\lambda x + Bsin\lambda x + Ccosh\lambda x + Dsinh\lambda x$$

In order to deal with this equation for the purpose of crack identification, the following assumptions are made

1. The crack is assumed open. This assumption is expected to be realistic because the crack is usually found in areas which are exposed to heavy weights, which naturally lead to an open crack. As a result of this assumption the crack is replaced by a torsional spring.

2. It is assumed that the crack is regular over the surface of the specimen, and uniform in propagation and found in one face of the sample.

3. Torsional spring is assumed to be at the clamped end, since the beam is partially restrained. This assumption consider gives a more accurate description of the restrained.

4. Shear deformation and Rotary inertia effects are ignored.

5. It is assumed that there are two amplitude functions for the cracked specimen, the first function represents the amplitude before the crack and the second represents the amplitude after the crack.

3.2 Crack Compliance

According to Rizos et al. [13], the crack compliance depends on the crack orientation and magnitude with respect to the main dimensions of cracked beam. Also it depends on applied loading and the mode of deformation. Dimarogonas [2] and Dimarogonas and Paipeties [3] calculated the crack compliance using the crack strain energy function. They found out that

$$K_T = \frac{1}{c} \tag{3.3}$$

$$c = (5.346h/EI)I(a/h)$$

Where c is the compliance,K_T is the bending spring constant, E is the modules of elasticity of the beam material, I is the moment of inertia of the beam cross-section and $I(a/h)$ is the dimensionless local compliance. It is derived for strain energy density functions and it is give by

$$I(a/h) = 1.8624(a/h)^2 - 3.95(a/h)^3 + 16.375(a/h)^4 - 37.226(a/h)^5$$

$$+76.81(a/h)^6 - 126.9(a/h)^7 + 172(a/h)^8 - 143.97(a/h)^9$$

$$+66.56(a/h)^{10}$$

3.3 Cracked Beam Mode

The crack is assumed to be open and to have uniform depth as shown in Figure 3.1. It is known that the modes of harmonic vibration apply on the two parts of the beam, left and right of the crack respectively. The equations of motion can be written as

$$\frac{d^4y_1}{dx^4} - \frac{\rho w^2}{EI}y_1 = 0 \qquad 0 \le x \le L_1 \tag{3.4}$$

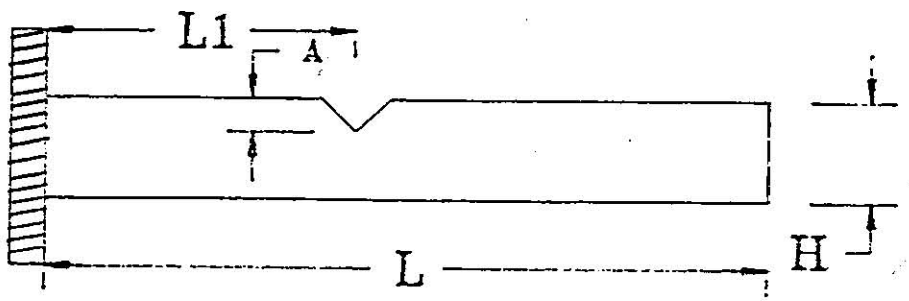

Figure 3.1: Cracked beam

$$\frac{d^4y_2}{dx^4} - \frac{\rho w^2}{EI}y_2 = 0 \qquad L_1 \leq x \leq L$$

The general solutions for these equations is

$$y_1(x) = A_1 sin\lambda x + B_1 cos\lambda x + C_1 sinh\lambda x + D_1 cosh\lambda x \tag{3.5}$$

$$y_2(x) = A_2 sin\lambda x + B_2 cos\lambda x + C_2 sinh\lambda x + D_2 cosh\lambda x \tag{3.6}$$

where

$$\lambda^4 = \frac{\rho w^2}{EI}$$

The coefficients in equations (3.5) and (3.6) are evaluated using the boundary conditions as shown in the next section.

3.4 Application Of The Boundary Conditions

To apply the boundary conditions, the beam is modeled using two springs. One at the clamped end to represent the restraint compliance. The second at the crack to represent the crack compliance. Consider Figure 3.2 for the boundary conditions application. The transverse displacement at the clamped end is stated as

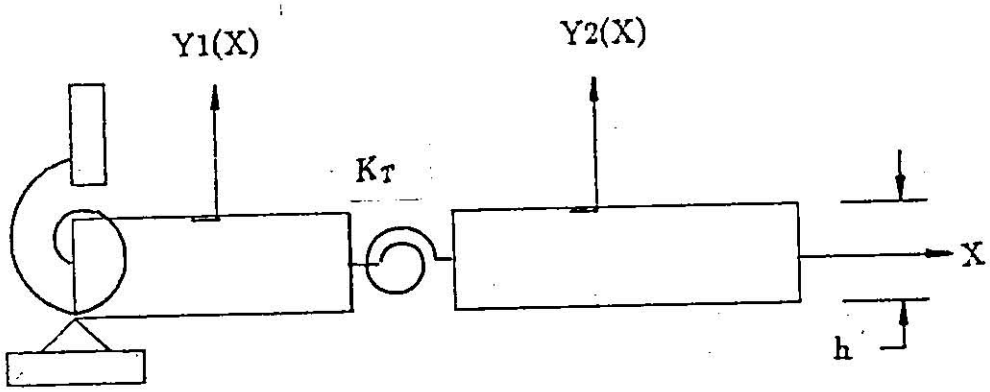

Figure 3.2: Analytical beam

$$y_1(0) = 0 \tag{3.7}$$

Substituting equation (3.7) into equation (3.5), leads to

$$B_1 = -D_1 \tag{3.8}$$

The rotation at the left end of the beam is partially restrained, therefore one can represent this condition by a torsional spring of stiffness K $\frac{N.m}{rad}$ as shown in figure 3.2. This condition can be written by expressing moment equilibrium at the left

$$EIy_1''(0) = Ky_1'(0) \tag{3.9}$$

Substituting equation (3.5) into equation (3.9), leads to

$$\frac{K}{EI\lambda}(A_1 + C_1) = D_1 - B_1 \tag{3.10}$$

Substituting equation (3.8) into equation (3.10), results in

$$\frac{K}{EI\lambda}(A_1 + C_1) = 2D_1$$

Solving for D_1, one obtains

$$D_1 = \frac{K}{2EI\lambda}(A_1 + C_1) \tag{3.11}$$

Substituting equations (3.11) and (3.7) into equation (3.5), one obtains

$$y_1(x) = A_1 sin\lambda x - \frac{K}{2EI\lambda}(A_1 + C_1)cos\lambda x \tag{3.12}$$

$$+C_1 sinh\lambda x + \frac{K}{2EI\lambda}(A_1 + C_1)cosh\lambda x$$

equation (3.12) can be rearranged as

$$y_1 = A_1(sin\lambda x + \frac{K}{2EI\lambda}(cosh\lambda x - cos\lambda x))+ \tag{3.13}$$

$$C_1(sinh\lambda x + \frac{K}{2EI\lambda}(cosh\lambda x - cos\lambda x))$$

At the free end of the beam, the moment must be zero, therefore

$$y_2''(L) = 0$$

Substituting this condition into equation (3.6), one obtains

$$\frac{dy_2}{dx} = \lambda A_2 cos\lambda x - \lambda B_2 sin\lambda x + \lambda C_2 cosh\lambda x + \lambda D_2 sinh\lambda x$$

$$\frac{d^2y_2}{dx^2} = -\lambda^2 A_2 sin\lambda x - \lambda^2 B_2 cos\lambda x + \lambda^2 C_2 sinh\lambda x + \lambda^2 D_2 cosh\lambda x$$

Substituting into $y_2''(L) = 0$, leads to

$$A_2 sin\lambda L + B_2 cos\lambda L = C_2 sinh\lambda L + B_2 cosh\lambda \tag{3.14}$$

At the free end of the beam the shear must be zero

$$y_2'''(L) = 0$$

Substituting this condition into equation (3.6), one obtains

$$\frac{d^3y_2}{dx^3} = -\lambda^3 A_2 cos\lambda x + \lambda^3 B_2 sin\lambda x + \lambda^3 C_2 cosh\lambda x + \lambda^3 D_2 sinh\lambda x$$

Substituting into $y_2'''(L) = 0$, one obtains

$$A_2 cos\lambda L = B_2 sin\lambda L + C_2 cosh\lambda L + D_2 sinh\lambda L \tag{3.15}$$

Substituting equation (3.15) into equation (3.14), leads to

$$B_2(sin\lambda L)^2 + C_2 cosh\lambda L sin\lambda L + D_2 sinh\lambda L sin\lambda L + B_2(cos\lambda L)^2$$

$$= C_2 sinh\lambda L cos\lambda L + D_2 cosh\lambda L cos\lambda L$$

solving for B_2, one obtains

$$B_2 = \frac{C_2(sinh\lambda L cos\lambda L - cosh\lambda L sin\lambda L)}{(sin\lambda L)^2 + (cos\lambda L)^2}$$

$$+\frac{D_2(cosh\lambda L cos\lambda L - sinh\lambda L sin\lambda L)}{(sin\lambda L)^2 + (cos\lambda L)^2}$$

For this equation, let

$$B_2 = \psi_1 C_2 + \psi_2 D_2 \tag{3.16}$$

where ψ_1 and ψ_2 are constants

Substituting equation (3.16) into equation (3.15) and solving for A_2, leads to

$$A_2 = (\psi_1 C_2 + \psi_2 D_2) tan\lambda L + C_2 \frac{cosh\lambda L}{cos\lambda L} + D_2 \frac{sinh\lambda L}{cos\lambda L}$$

$$A_2 = \left(\psi_1 \frac{sin\lambda L}{cos\lambda L} + \frac{cosh\lambda L}{cos\lambda L}\right) C_2 + \left(\psi 2 \frac{sin\lambda L}{cos\lambda L} + \frac{sinh\lambda L}{cos\lambda L}\right) D_2$$

For the last relation, let

$$A_2 = \psi_3 C_2 + \psi_4 D_4 \tag{3.17}$$

Whereψ_3 and ψ_4 are constants

substituting equation (3.16) and equation (3.17) into equation (3.6), leads to

$$y_2(x) = (\psi_3 C_2 + \psi_4 D_2) sin\lambda x + (\psi_1 C_2 + \psi_2 D_2) cos\lambda x$$

$$+C_2 sinh\lambda x + D_2 cosh\lambda x$$

This equation can be rearranged as

$$y_2(x) = (\psi_1 cos\lambda x + \psi_3 sin\lambda x + sinh\lambda x)C_2 \tag{3.18}$$

$$+(\psi_2 cos\lambda x + \psi_4 sin\lambda x + cosh\lambda x)D_2$$

As shown in figure 3.2 the deflection condition at the crack location is

$$y_1(L_1) = y_2(L_1)$$

Substituting equation (3.13) and equation (3.18) into this condition, one obtains

$$A_1(sin\lambda L_1 + \frac{K}{2EI\lambda}(cosh\lambda L_1 - cos\lambda L_1))+$$

$$C_1(sinh\lambda L_1 + \frac{K}{2EI\lambda}(cosh\lambda L_1 - cos\lambda L_1))$$

$$= (\psi_1 cos\lambda L_1 + \psi_3 sin\lambda L_1 + sinh\lambda L_1)C_2$$

$$(\psi_2 cos\lambda L_1 + \psi_4 sin\lambda L_1 + cosh\lambda L_1)D_2$$

Rearrange this equation as

$$D_2 = \left(\frac{sin\lambda L_1 + \frac{K}{2EI\lambda}(cosh\lambda L_1 - cos\lambda L_1)}{\psi_2 cos\lambda L_1 + \psi_4 sin\lambda L_1 + cosh\lambda L_1}\right) A_1 \tag{3.19}$$

$$+\left(\frac{sinh\lambda L_1 + \frac{K}{2EI\lambda}(cosh\lambda L_1 - cos\lambda L_1)}{\psi_2 cos\lambda L_1 + \psi_4 sin\lambda L_1 + cosh\lambda L_1}\right) C_1$$

$$-\left(\frac{\psi_1 cos\lambda L_1 + \psi_3 sin\lambda L_1 + sinh\lambda L_1}{\psi_2 cos\lambda L_1 + \psi_4 sin\lambda L_1 + cosh\lambda L_1}\right) C_2$$

From compatibility condition for rotation of flexibility,

$$y_1{\prime}(L_1) + \frac{EI}{K_T} y_1{\prime\prime}(L_1) = y_2{\prime}(L_1)$$

Substituting equation (3.13) and equation (3.18) into this condition, one obtains

$$\lambda A_1(cos\lambda L_1 + \frac{K}{2EI\lambda}(sinh\lambda L_1 + sin\lambda L_1))$$

$$+\lambda C_1(cosh\lambda L_1 + \frac{K}{2EI\lambda}(sinh\lambda L_1 + sin\lambda L_1))$$

$$(\frac{\lambda^2 E}{K_T})(A_1(-sin\lambda L_1 + \frac{K}{2EI\lambda}(cosh\lambda L_1 + cos\lambda L_1))$$

$$+C_1(sinh\lambda L_1 + \frac{K}{2EI\lambda}(cosh\lambda L_1 + cos\lambda L_1)))$$

$$= \lambda(-\psi_1 sin\lambda L_1 + \psi_3 cos\lambda L_1 + cosh\lambda L_1)C_2$$

$$+\lambda(-\psi_2 sin\lambda L_1 + \psi_4 cos\lambda L_1 + sinh\lambda L_1)D_2$$

From this equation one obtains

$$D_2 = \left(\frac{cos\lambda L_1 + \frac{K}{2EI\lambda}(sinh\lambda L_1 + sin\lambda L_1)}{-\psi_2 sin\lambda L_1 + \psi_4 cos\lambda L_1 + sinh\lambda L_1}\right) A_1 \qquad (3.20)$$

$$+\left(\frac{(\frac{\lambda EI}{K_T})(-sin\lambda L_1 + \frac{K}{2EI\lambda}(cosh\lambda L_1 + cos\lambda L_1)}{-\psi_2 sin\lambda L_1 + \psi_4 cos\lambda L_1 + sinh\lambda L_1}\right) A_1$$

$$+\left(\frac{cosh\lambda L_1 + \frac{K}{2EI\lambda}(sinh\lambda L_1 + sin\lambda L_1)}{-\psi_2 sin\lambda L_1 + \psi_4 cos\lambda L_1 + sinh\lambda L_1}\right) C_1$$

$$+\left(\frac{(\frac{\lambda EI}{K_T})(sinh\lambda L_1 + \frac{K}{2EI\lambda}(cosh\lambda L_1 + cos\lambda L_1))}{-\psi_2 sin\lambda L_1 + \psi_4 cos\lambda L_1 + sinh\lambda L_1}\right) C_1$$

$$-\left(\frac{-\psi_1 sin\lambda L_1 + \psi_3 cosh\lambda L_1 + cosh\lambda L_1}{-\psi_2 sin\lambda L_1 + \psi_4 cos\lambda L_1 + sinh\lambda L_1}\right) C_2$$

Equation (3.20) and equation (3.19), leads to

$$\left(\frac{A_1(sin\lambda L_1 + \frac{K}{2EI\lambda}(cosh\lambda L_1 - cos\lambda L_1))}{\psi_2 cos\lambda L_1 + \psi_4 sin\lambda L_1 + cosh\lambda L_1}\right)$$

$$+\left(\frac{C_1(sinh\lambda L_1 + \frac{K}{2EI\lambda}(cosh\lambda L_1 - cos\lambda L_1))}{\psi_2 cos\lambda L_1 + \psi_4 sin\lambda L_1 + cosh\lambda L_1}\right)$$

$$-\left(\frac{\psi_1 cos\lambda L_1 + \psi_3 sin\lambda L_1 + sinh\lambda L_1}{\psi_2 cos\lambda L_1 + \psi_4 sin\lambda L_1 + cosh\lambda L_1}\right) C_2$$

$$= \left(\frac{cos\lambda L_1 + \frac{K}{2EI\lambda}(sinh\lambda L_1 + sin\lambda L_1)}{-\psi_2 sin\lambda L_1 + \psi_4 cos\lambda L_1 + sinh\lambda L_1}\right) A_1$$

$$+\left(\frac{(\frac{\lambda EI}{K_T})(-sin\lambda L_1 + \frac{K}{2EI\lambda}(cosh\lambda L_1 + cos\lambda L_1)}{-\psi_2 sin\lambda L_1 + \psi_4 cos\lambda L_1 + sinh\lambda L_1}\right) A_1$$

$$+\left(\frac{cosh\lambda L_1 + \frac{K}{2EI\lambda}(sinh\lambda L_1 + sin\lambda L_1)}{-\psi_2 sin\lambda L_1 + \psi_4 cos\lambda L_1 + sinh\lambda L_1}\right) C_1$$

$$+\left(\frac{(\frac{\lambda EI}{K_T})(sinh\lambda L_1+\frac{K}{2EI\lambda}(cosh\lambda L_1+cos\lambda L_1))}{-\psi_2 sin\lambda L_1+\psi_4 cos\lambda L_1+sinh\lambda L_1}\right)C_1$$

$$-\left(\frac{-\psi_1 sin\lambda L_1+\psi_3 cosh\lambda L_1+cosh\lambda L_1}{-\psi_2 sin\lambda L_1+\psi_4 cos\lambda L_1+sinh\lambda L_1}\right)C_2$$

For this equation, let

$$\eta_1 A_1+\eta_2 C_1+\eta_3 C_2=\eta_4 A_1+\eta_5 A_1 \tag{3.21}$$

$$+\eta_6 C_1+\eta_7 C_1+\eta_8 C_2$$

Where η_i(i=1,...8) are constants

Solving for C_2 from equation (3.21), one obtains

$$C_2=\left(\frac{A_1(\eta_1-\eta_4-\eta_5)+C_1(\eta_2-\eta_6-\eta_7)}{\eta_8-\eta_3}\right)$$

For this equation, let

$$C_2=\psi_5 A_1+\psi_6 C_1 \tag{3.22}$$

Where ψ_5 and ψ_6 are constants.

Substituting equation (3.22) into equation (3.19), one obtains

$$D_2=\left(\frac{sin\lambda L_1+\frac{K}{2EI\lambda}(cosh\lambda L_1-cos\lambda L_1)}{\psi_2 cos\lambda L_1+\psi_4 sin\lambda L_1+cosh\lambda L_1}\right)A_1$$

$$+\left(\frac{sinh\lambda L_1+\frac{K}{2EI\lambda}(cosh\lambda L_1-cos\lambda L_1)}{\psi_2 cos\lambda L_1+\psi_4 sin\lambda L_1+cosh\lambda L_1}\right)C_1$$

$$-\left(\frac{\psi_1 cos\lambda L_1+\psi_3 sin\lambda L_1+sinh\lambda L_1}{\psi_2 cos\lambda L_1+\psi_4 sin\lambda L_1+cosh\lambda L_1}\right)(\psi_5 A_1+\psi_6 C_1)$$

From this equation, one obtains

$$D_2=A_1\left(\frac{sin\lambda L_1+\frac{K}{2EI\lambda}(cosh\lambda L_1-cos\lambda L_1)}{\psi_2 cos\lambda L_1+\psi_4 sin\lambda L_1+cosh\lambda L_1}\right)$$

$$-\left(\frac{\psi_1 cos\lambda L_1+\psi_3 sin\lambda L_1+sinh\lambda L_1}{\psi_2 cos\lambda L_1+\psi_4 sin\lambda L_1+cosh\lambda L_1}(\psi_5)\right)$$

$$+C_1\left(\frac{sinh\lambda L_1+\frac{K}{2EI\lambda}(cosh\lambda L_1-cos\lambda L_1)}{\psi_2 cos\lambda L_1+\psi_4 sin\lambda L_1+cosh\lambda L_1}\right)$$
$$-\left(\frac{\psi_1 cos\lambda L_1+\psi_3 sin\lambda L_1+sinh\lambda L_1}{\psi_2 cos\lambda L_1+\psi_4 sin\lambda L_1+cosh\lambda L_1}(\psi_6)\right)$$

For this equation, let

$$D_2=\psi_7 A_1+\psi_8 C_1 \tag{3.23}$$

Where ψ_7 and ψ_8 are constants

Substituting equation (3.22) and equation (3.23) into equation (3.18), leads to

$$y_2(x)=(\psi_1 cos\lambda x+\psi_3 sin\lambda x+sinh\lambda x)(\psi_5 A_1+\psi_6 C_1)$$

$$+(\psi_2 cos\lambda x+\psi_4 sin\lambda x+cosh\lambda x)(\psi_7 A_1+\psi_8 C_1)$$

From this equation one obtains

$$y_2(x)=A_1\left[\psi_5(\psi_1 cos\lambda x+\psi_3 sin\lambda x+sinh\lambda x)\right. \tag{3.24}$$

$$\left.+\psi_7(\psi_2 cos\lambda x+\psi_4 sin\lambda x+cosh\lambda x)\right]$$

$$+C_1\left[\psi_6(\psi_1 cos\lambda x+\psi_3 sin\lambda x+sinh\lambda x)\right)$$

$$\left.+\psi_8(\psi_2 cos\lambda x+\psi_4 sin\lambda x+cosh\lambda x)\right]$$

Moment Equation at the crack location as shown in figure 3.2 is

$$EIy_1''(L_1)=EIy_2''(L_1)$$

Substituting equation (3.13) and equation (3.24) into this condition, one obtains

$$EI\lambda^2((-sin\lambda L_1+\frac{K}{2EI\lambda}(cosh\lambda L_1+cos\lambda L_1))A_1$$

$$+C_1(sinh\lambda L_1+\frac{K}{2EI\lambda}(cosh\lambda L_1+cos\lambda L_1)))$$

$$=EI\lambda^2 A_1\left(\psi_5(-\psi_1 cos\lambda L_1-\psi_3 sin\lambda L_1+sinh\lambda L_1)\right.$$

$$\left.+\psi_7(-\psi_2 cos\lambda L_1-\psi_4 sin\lambda L_1+cosh\lambda L_1)\right)$$

$$+C_1\,(\psi_6(-\psi_1 cos\lambda L_1 - \psi_3 sin\lambda L_1 + sinh\lambda L_1)$$

$$+\psi_8(-\psi_2 cos\lambda L_1 - \psi_4 sin\lambda L_1 + cosh\lambda L_1))$$

Solving this equation for A_1 and C_1, one obtains

$$A_1(-sin\lambda L_1 + \frac{K}{2EI\lambda}(cosh\lambda L_1 + cos\lambda L_1)$$

$$-\psi_5(-\psi_1 cos\lambda L_1 - \psi_3 sin\lambda L_1 + sinh\lambda L_1)$$

$$-\psi_7(-\psi_2 cos\lambda L_1 - \psi_4 sin\lambda L_1 + cosh\lambda L_1))$$

$$+C_1(sinh\lambda L_1 + \frac{K}{2EI\lambda}(cosh\lambda L_1 + cos\lambda L_1)$$

$$-\psi_6(-\psi_1 cos\lambda L_1 - \psi_3 sin\lambda L_1 + sinh\lambda L_1)$$

$$-\psi_8(-\psi_2 cos\lambda L_1 - \psi_4 sin\lambda L_1 + cosh\lambda L_1)) = 0$$

For this equation, let

$$\psi_9 A_1 + \psi_{10} C_1 = 0 \tag{3.25}$$

Where ψ_9 and ψ_{10} are constants

Shear compatibility equation at the crack location as shown in figure 3.2 is given by

$$EIy_1'''(L_1) = EIy_2'''(L_1)$$

Substituting equations (3.13) and (3.24) into this condition, leads to

$$EI\lambda^3((-cos\lambda L_1 + \frac{K}{2EI\lambda}(sinh\lambda L_1 - sin\lambda L_1))A_1$$

$$+C_1(cosh\lambda L_1 + \frac{K}{2EI\lambda}(sinh\lambda L_1 - sin\lambda L_1)))$$

$$= EI\lambda^3 A_1\,(\psi_5(\psi_1 sin\lambda L_1 - \psi_3 cos\lambda L_1 + cosh\lambda L_1)$$

$$+\psi_7\,(\psi_2 sin\lambda L_1 - \psi_4 cos\lambda L_1 + sinh\lambda L_1))$$

$$+C_1(\psi_6(\psi_1 sin\lambda L_1 - \psi_3 cos\lambda L_1 + cosh\lambda L_1)$$

$$+\psi_8\,(\psi_2 sin\lambda L_1 - \psi_4 cos\lambda L_1 + sinh\lambda L_1))$$

Solving this equation for A_1 and C_1 one obtains

$$A_1(-cos\lambda L_1 + \frac{K}{2EI\lambda}(sinh\lambda L_1 - sin\lambda L_1)$$

$$-\psi_5(\psi_1 sin\lambda L_1 - \psi_3 cos\lambda L_1 + cosh\lambda L_1)$$

$$-\psi_7(\psi_2 sin\lambda L_1 - \psi_4 cos\lambda L_1 + sinh\lambda L_1))$$

$$+C_1(cosh\lambda L_1 + \frac{K}{2EI\lambda}(sinh\lambda L_1 - sin\lambda L_1)$$

$$-\psi_6(\psi_1 sin\lambda L_1 - \psi_3 cos\lambda L_1 + cosh\lambda L_1)$$

$$-\psi_8(\psi_2 sin\lambda L_1 - \psi_4 cos\lambda L_1 + sinh\lambda L_1)) = 0$$

For this equation, let

$$\psi_{11} A_1 + \psi_{12} C_1 = 0 \tag{3.26}$$

Where ψ_{11} and ψ_{12} are constant

From equation (3.25) and equation (3.26), one obtains

$$\psi_9 A_1 + \psi_{10} C_1 = 0$$

$$\psi_{11} A_1 + \psi_{12} C_1 = 0 \tag{3.27}$$

Writing the last equation in matrix form, leads to

$$\begin{bmatrix} \psi_9 & \psi_{10} \\ \psi_{11} & \psi_{12} \end{bmatrix} \begin{bmatrix} A_1 \\ C_1 \end{bmatrix} = \begin{bmatrix} 0 \\ 0 \end{bmatrix} \tag{3.28}$$

Equation (3.28) is a singular equation, therefore A_1 and C_1 can not be zero, so

$$\psi_9 \psi_{12} - \psi_{11} \psi_{10} = 0 \tag{3.29}$$

Equation (3.29) is function of crack depth, crack location, and frequency , therefore for known depth and location of the crack, the frequency for each mode can be estimated. Program II was developed to solve this equation , this will be discussed in Chapter V.

Chapter 4

EXPERIMENTAL SET-UP

In this chapter the apparatus employed in the present study will be described in detail. The various components that constitute the whole system are illustrated. The preparation of the specimens, their fastening to the system, and data recording and processing are explained herein.

4.1 Apparatus

The system used in this study consists of the following devices: Exciter, Measuring amplifier, Oscilloscope, Amplifier, Power supply, Vibration meter, Exciter controller, Magnetic Transducer, and Accelerometer. These devices are described in the following.

1. Exciter: The exciter of type 4808 B&K was used in this test. The specimens were fastened on the exciter by a clamping Aluminum piece by four bolts as shown in Figure 4.1. The desired frequency for the exciter is attained by the aid of the exciter controller which also was used to change the frequency from a certain value to another in order to study the effect of crack and slot on the natural mode of the specimens. This exciter is shown in Figure 4.2

2. Oscilloscope: The output signal was obtained using a digital oscilloscope of type HP 54501A Digitizing Oscilloscope. This Oscilloscope has been

designed for ease-of-use with easy-to-find control keys. This device is very accurate, sensitive, and reliable. Through the observation of the behavior of the signal output on the screen, it is known that at the resonance (first mode, second mode,...etc) of a certain specimen, a jump will occur in the output signal. The device is shown in Figure 4.3.

3. Exciter Controller: Exciter Controller type 1047 B & K was used to control the input frequencies to the Exciter, it is shown in Figure 4.4

4. Measuring Amplifier: The B & K measuring amplifier type 2610 was used to measure and filter the signal coming from the transducer before it was introduced to the oscilloscope, it is shown in Figure 4.5

5. Vibration Meter: Vibration meter type 2511 B & K was used in the measurement and monitoring of vibration levels on the specimens used in this study. It is shown in Figure 4.6

6. Magnetic Transducer: The Magnetic Transducer type MM0002 was moved along the beam to measure the mode amplitude. This transducer was connected to the measuring amplifier to transmit the output signal to the oscilloscope screen. It is shown in Figure 4.7

7. Accelerometer: The Accelerometer type 4370 B & K was kept at the clamped end of the beam to give the reference input. It is shown in Figure 4.8

8. Power Supply: The vibration meter was connected to a power supply type 2808 B & K . it is shown in Figure 4.9

9. Power Amplifier: The exciter was connected to the power amplifier type 2712 B & K, to amplify the power input to the exciter.

4.2 Experimental Set-Up

The previous devices were connected to each other as shown in Figure 4.10 and Figure 4.11. The data acquisition from this set-up is explained in section 4.4

4.3 Specimens Preparation

Mild steel with dimensions 9.9mmx9.9mmx201mm specimens were used in this study. The specimens were tested in the Royal Scientific Society. The test revealed that the modules of elasticity is 200 Gpa and the yield stress is 554 Mpa. A stress-strain diagram for the tested specimen is shown in Figure 4.12. In addition, a chemical test was performed in order to know the chemical composition of the specimen, the test revealed that the specimen is made of the constituent shown in Table 4.1 with indicated percentage.

A crack was introduced in four different specimens at different locations. The crack was initiated by a slot less than .5mm in depth at the desired location. The specimen was clamped up to the slot and a dynamic load was imposed at the other end of the specimen. The maximum bending will be, as result, at the slot. A lathe machine was used to clamp one end of the specimen, while the other end of the specimen was fitted inside a ball bearing. A radial load was applied at the bearing using the tool holder. the lathe machine was operated at a certain speed until fracture takes place. The number of revolutions needed to fracture the specimen is determined. Therefore, this experiment was repeated but with lesser number of revolutions in order to propagate the initial crack.

This method is purely a practical one, it exactly resembles the " Trial and Error" method, since various specimens were destroyed in order to get a cracked specimen.

Table 4.1: Specimens Constituent

Constituent	Percentage %
C	0.14%
Si	0.25%
Mn	0.79%
Mo	0.66%
Ni	0.16%

It is obvious that the crack is out of control with respect to propagation and depth. In order to make this study clearer and closer to theory, slots were made, by milling machine using a .5mm cutting tool. This was done for different locations and various depths.

4.4 Performing the test

Each specimen was clamped separately on the exciter where 41mm of each specimen was inserted in the Aluminum clamping piece. Consequently, a cantilever with 9.9mmx9.9mmx160mm dimensions was obtained.

After the system was operated, the frequency was changed by the aid of exciter controller. The transducer was moved along the specimen to get the mode shape and the natural frequency at resonance excitation. Resonance frequency was detected by observing the change in the amplitude at the oscilloscope screen. At resonance the change in amplitude is sudden and easily observed.

Initially, uncracked beam was tested. The first mode shape and its corresponding natural frequency were found. This experiment was repeated for the cracked specimens, where the change in mode shape and natural frequency were observed.

The vibration amplitude at the first mode was measured at 10mm- steps, starting

from the clamped end of the beam. The amplitude is measured by the transducer type MM0002 mounted three millimeters above the beam. The value of the amplitude at the tip and at the clamped end were obtained using interpolation, since it is difficult to have a reading at these two locations. The normalized non-dimensional mode shape was obtained using the relation.

$$V_n = \frac{V - V_c}{V_t - V_c}$$

Where V_n is the normalized voltage, V is the measured voltage along the beam, V_t is the maximum measured voltage which equal to the voltage at the tip of the specimens, and V_c is the voltage at the clamped end.

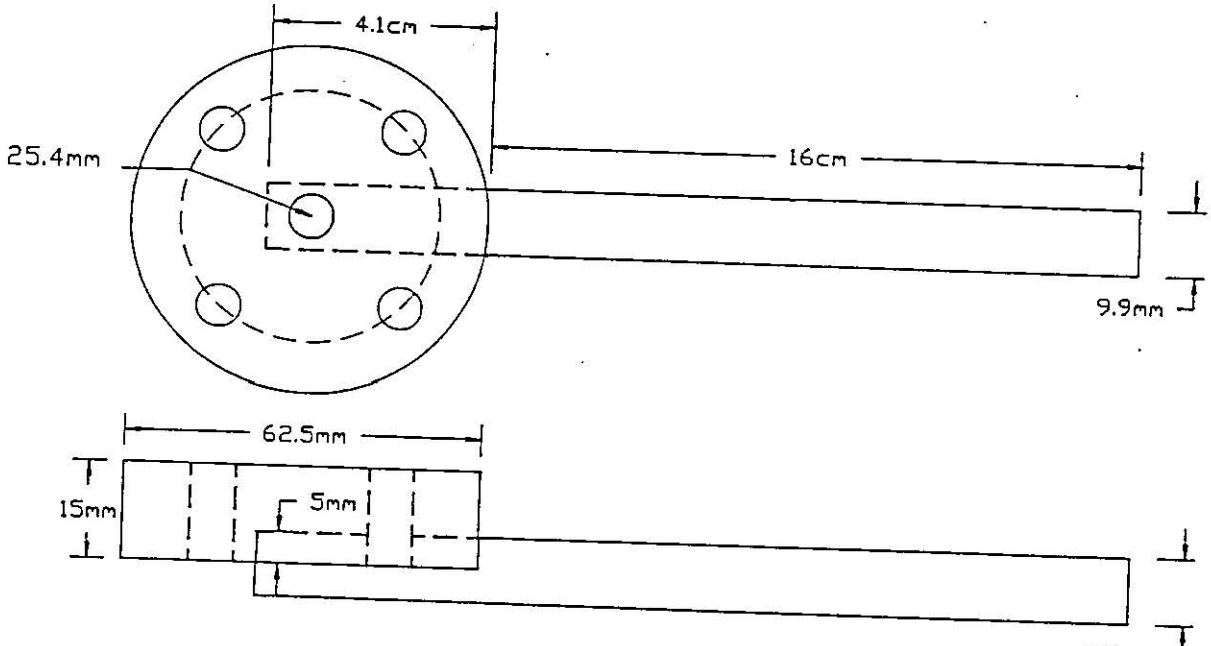

Figure 4.1: Aluminum piece for fixing purposes

Figure 4.2: Exciter type 4808 B&K

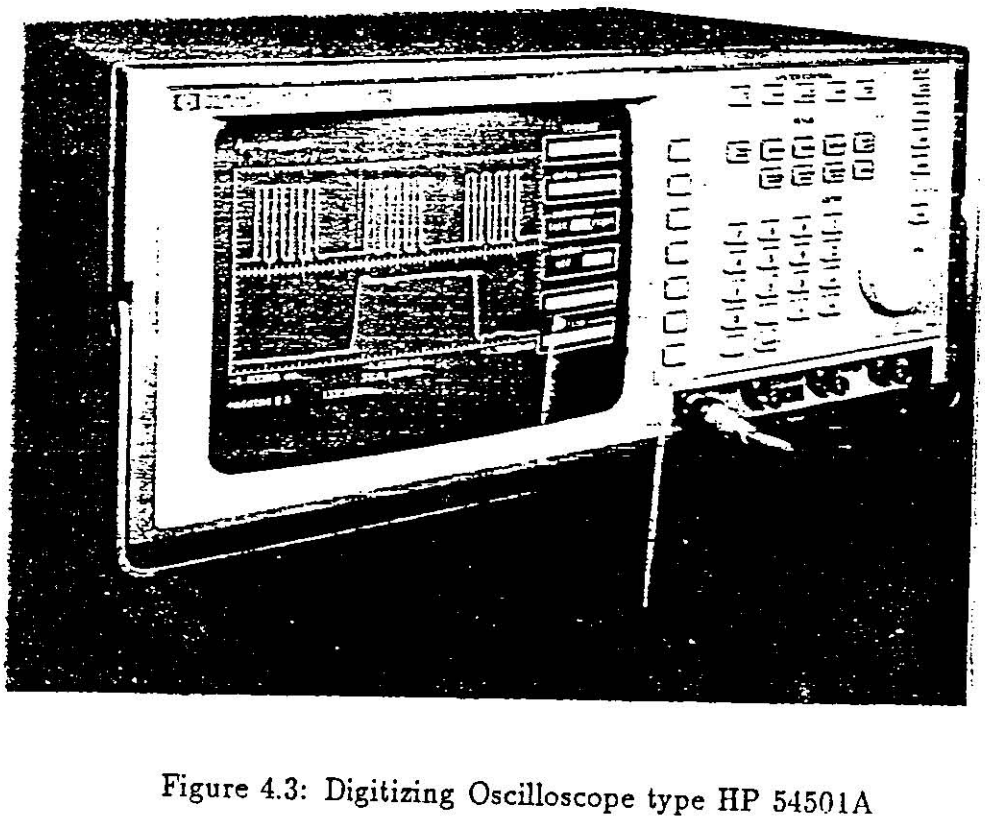

Figure 4.3: Digitizing Oscilloscope type HP 54501A

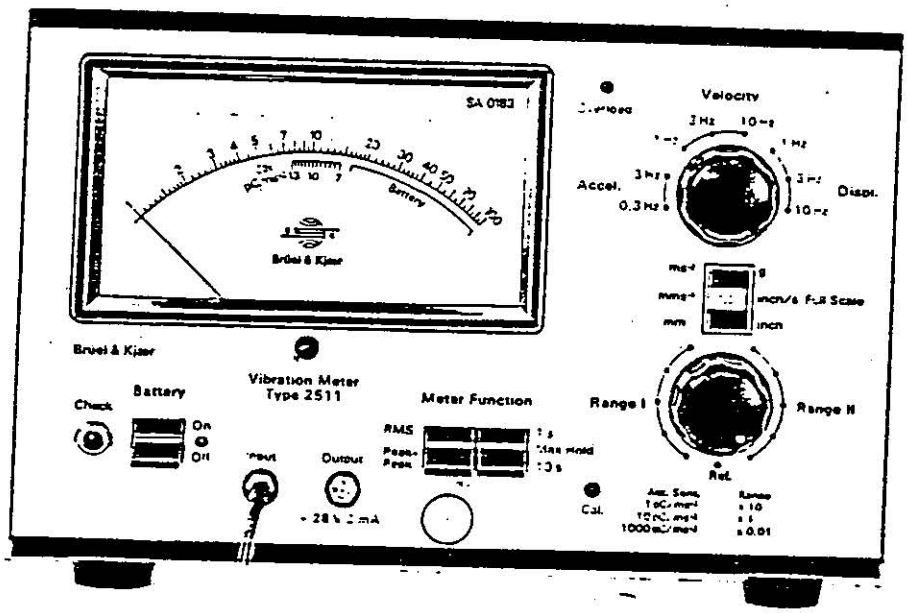

Figure 4.6: Vibration Meter type 2511 B & K

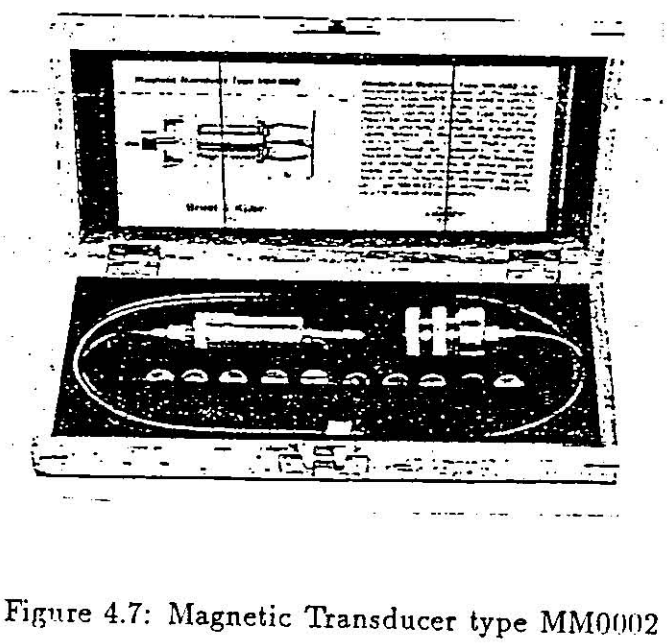

Figure 4.7: Magnetic Transducer type MM0002

Figure 4.8: Accelerometer type 4370 B & K

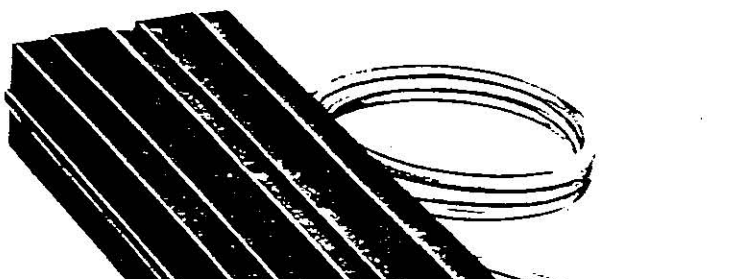

Figure 4.9: Power Supply type 2808 B & K

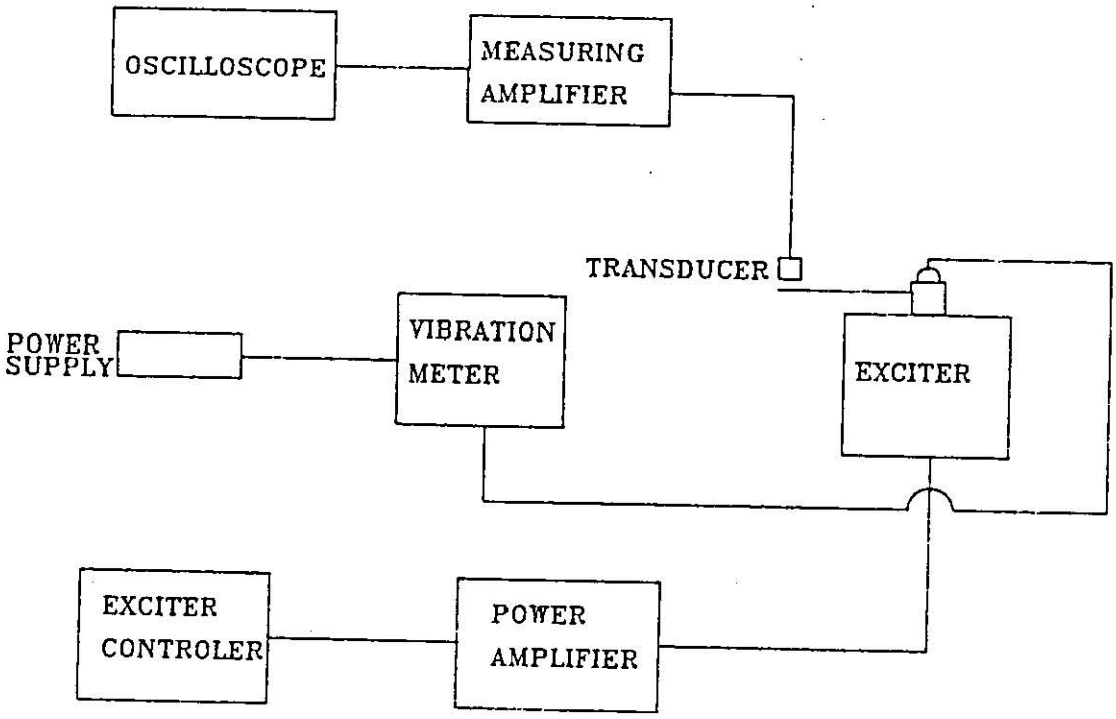

Figure 4.10: Measurement System

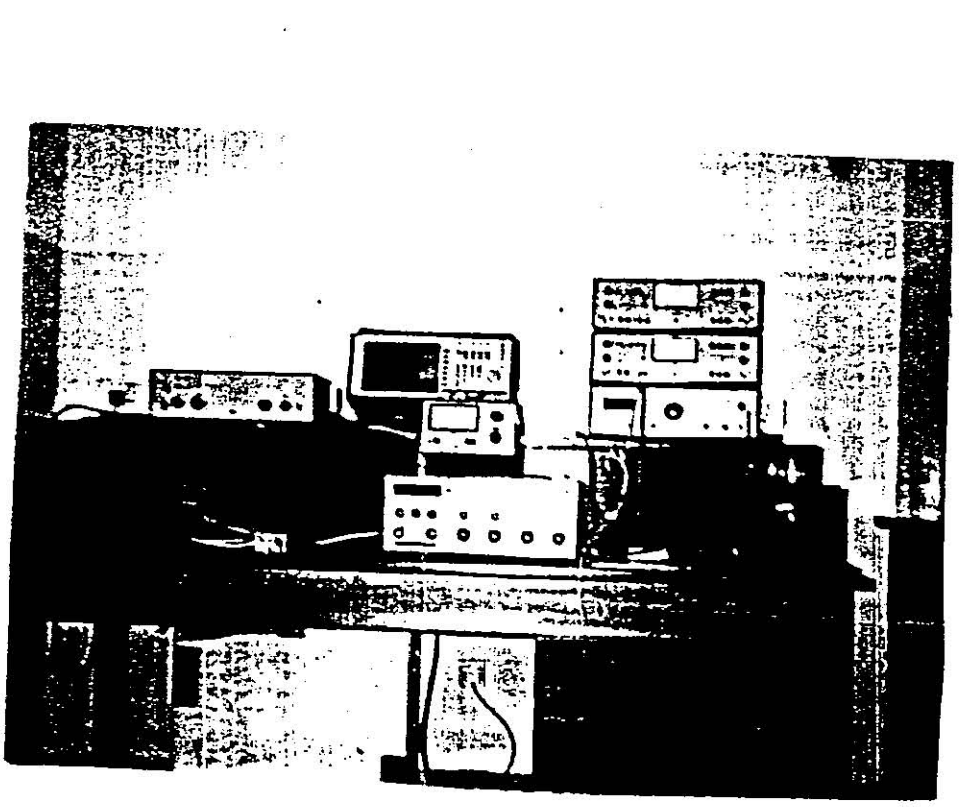

Figure 4.11: Measurement System

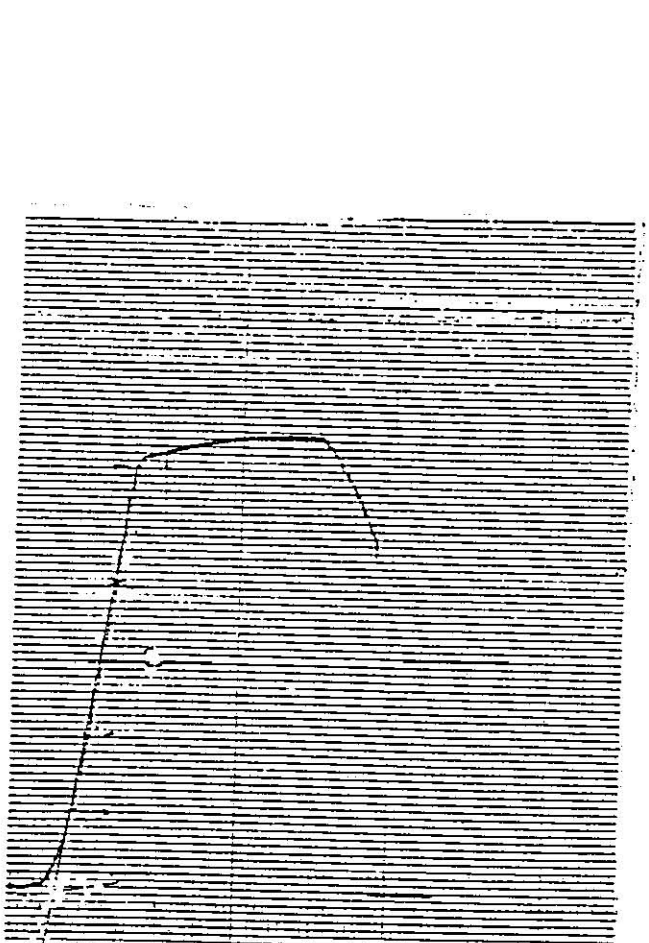

Figure 4.12: stress strain relation

Chapter 5

RESULTS AND DISCUSSION

In this chapter the experimental results are analyzed. The effects of the crack on the dynamic response are studied so that a relations between these effects and the crack parameters are obtained.

The experimental results are utilized in evaluating the spring constant representing the compliance at the clamped end. This spring constant value is used back in the theoretical equations in order to obtain accurate values for the natural frequencies and mode shapes. For this reason , the evaluation of this constant is done first.

The conclusions drawn from the analyses of the expetimental results show that the method developed by Rizos [15] has some faults.

5.1 Evaluation Of The Spring Constant At The Clamped End

It is noticed that, as a result of using four bolts to fasten the specimens, a reduction in frequency band of uncracked specimen with respect to cantilever had taken place. It is found that this method of fastening tends to partially restrains the end. To compensate for this compliance, a bending spring is utilized to theoretically model it. The value of this spring constant is evaluated using the experimental value

Applying boundary conditions in evaluating A, B, C, and D results in

$$\begin{bmatrix} \beta_1 & \beta_2 \\ \beta_3 & \beta_4 \end{bmatrix} \begin{bmatrix} A \\ C \end{bmatrix} = \begin{bmatrix} 0 \\ 0 \end{bmatrix} \tag{5.3}$$

Where

$$\beta_1 = \frac{K}{2EI\lambda}(cosh\lambda L + cos\lambda L) - sin\lambda L$$

$$\beta_2 = \frac{K}{2EI\lambda}(cosh\lambda L + cos\lambda L) + sinh\lambda L$$

$$\beta_3 = \frac{K}{2EI\lambda}(sinh\lambda L - sin\lambda L) - cos\lambda L$$

$$\beta_4 = \frac{K}{2EI\lambda}(sinh\lambda L - sin\lambda L) + cosh\lambda L$$

A and C can not be zero. Therefore

$$\begin{vmatrix} \beta_1 & \beta_2 \\ \beta_3 & \beta_4 \end{vmatrix} = 0 \tag{5.4}$$

Leading to an additional equation to evaluate the value of K. It could be shown that K is given by

$$K = \frac{sin\lambda L cos\lambda L - sinh\lambda L cos\lambda L}{A_1 cosh\lambda L - A_2 sin\lambda L + A_3 cos\lambda L - A_4 sinh\lambda L cosh\lambda L} \tag{5.5}$$

Where

$$A_1 = \frac{cosh\lambda L + cos\lambda L}{2EI\lambda}$$

$$A_2 = \frac{sinh\lambda L - sin\lambda L}{2EI\lambda}$$

$$A_3 = \frac{cosh\lambda L + cos\lambda L}{2EI\lambda}$$

$$A_4 = \frac{sinh\lambda L - sin\lambda L}{2EI\lambda}$$

Program I is used to evaluate the value of K for any value of λ which is given by

$$\lambda^4 = \frac{\rho w^2}{EI}$$

Where ρ, and EI are constants, which means that the value of K at constant ρ and EI is dependent on the value of ω only, where

$$w = 2\pi F$$

In which F is the frequency in Hz, this frequency is found experimentally for uncrack beam specimen. It was found that the fundamental frequency is at 275 Hz substituting this value in equation (5.5). It was found that

$$K = 13775.93 \frac{N.m}{rad.}$$

In Figure 5.2 the value of K is plotted against the frequency. It could be noticed that the value of K approaches infinity when the value of frequency approaches the first fundamental natural frequency af a theoretical cantilever beam.

5.2 Mode Detection

The non-linear equation for known crack characteristics (location and depth) is given by

$$\begin{vmatrix} \psi_9 & \psi_{10} \\ \psi_{11} & \psi_{12} \end{vmatrix} = 0 \qquad (5.6)$$

Equation 5.6 was derived in chapter 3. This equation is used to evaluate natural frequency using program II, which was developed for this purpose. Table (5.1) shows both experimental and theoretical values for frequencies for a number of specimens which have slots at a fixed distance of 3cm and at various depths. Table (5.2) shows the experimental and theoretical values for a number of specimens that have slots at depth of 3mm and at various locations. It is found that a reduction in frequency for the first mode is taken place as a result of crack. This reduction is shown in table (5.3) and Fig.(5.3) theoretically, and experimentally for a specimens with slot at a distance 3cm and different depth. It is obvious that the reduction in the frequency, of the first mode, increases with the increase in the slot depth. Table (5.4) and Fig.(5.4) shows the predicted reduction and measured reduction, for specimens which have slots at a depth of 3mm and different locations. It is observed that the reduction in frequency for specimens which have slots close to the clamped end, more than the specimens which have remote slots from the clamped end. Table (5.5) shows the theoretical and experimental values of the frequencies at the first mode for four specimens which have cracks instead of slots at different locations. For two of these four beams the theoretical values are not listed for reason to be discussed in section 5.5. Table (5.6) shows that the crack close to the clamped end has an effect on the natural frequency of the first mode more than the remote one.

Table 5.1: Frequency of the first mode for slots at 3cm location (Hz)

Slot depth mm	Theoretical	Experimental
0	275	275
1	273.854	274.2
3	264.622	268.5
5	242.34187	247.3
7	191.08579	202.7
8	150.48886	167.3

Table 5.2: Frequency of the first mode for slots at 3mm depth and different location (Hz)

Slot location cm	Theoretical	Experimental
1	259.5279	263.1
2	262.18626	265.3
3	264.622	268.5
4	266.8145	269.8
5	268.7446	271.4
6	270.39873	272.2
7	271.7709	273.1
8	272.8657	274.1

Table 5.3: Reduction in Frequency according to slots at 3cm location and different depth

Slot depth mm	Reduction in Theor.	Reduction in Exp..
0	0	0
1	0.416%	0.29%
3	3.77%	2.36%
5	11.87%	10.07%
7	30.514%	26.29%
8	45.27%	39.16%

Table 5.4: Reduction in Frequency according to slots at 3mm depth and different locations

Slot location cm	Reduction in Theor.	Reduction in Exp.
1	5.6%	4.32%
2	4.66%	3.52%
3	3.77%	2.36%
4	2.97%	1.89%
5	2.27%	1.31%
6	1.67%	1%
7	1.17%	0.69%
8	0.776%	0.32%

Table 5.5: Frequency of the first mode for cracks at different depth and different location (Hz)

Crack location cm	Theoretical	Experimental
1	261.8634	266.7
3	267.5906	271.3
5	—	273.2
6	—	272.8

Table 5.6: Reduction in Frequency according to crack at different depths and different locations

Crack location cm	Reduction in Theor.	Reduction in Exp.
1	4.77%	3%
3	2.69%	1.34%
5	—%	0.65%
6	—%	0.8%

5.3 Dynamic Behaviour Of Uncracked Beam

The vibration modes of the uncracked beam is modeled by equation (3.13) and equation (3.24). These equations are written as

$$y_1(x) = A_1(sin\lambda x + \frac{K}{2EI\lambda}(cosh\lambda x - cos\lambda x))+ \quad (5.7)$$
$$C_1(sinh\lambda x + \frac{K}{2EI\lambda}(cosh\lambda x - cos\lambda x))$$

$$0 \leq x \leq L_1$$

$$y_2(x) = A_1\,[\psi_5(\psi_1 cos\lambda x + \psi_3 sin\lambda x + sinh\lambda x)) \quad (5.8)$$

$$+\psi_7\,(\psi_2 cos\lambda x + \psi_4 sin\lambda x + cosh\lambda x)]$$

$$+C_1\,[\psi_6(\psi_1 cos\lambda x + \psi_3 sin\lambda x + sinh\lambda x))$$

$$+\psi_8\,(\psi_2 cos\lambda x + \psi_4 sin\lambda x + cosh\lambda x)]$$

$$L_1 \leq x \leq L$$

To model cracked beams, the crack depth is considered to approach zero or L_1 is equal to L to model uncracked beam. The value of bending spring constant K at the clamped end is utilized. Equation (5.7) and equation (5.8) are divided by C_1, leading to

$$\frac{y_1(x)}{C_1} = \frac{A_1}{C_1}(sin\lambda x + \frac{K}{2EI\lambda}(cosh\lambda x - cos\lambda x))+ \qquad (5.9)$$
$$(sinh\lambda x + \frac{K}{2EI\lambda}(cosh\lambda x - cos\lambda x))$$

$$0 \leq x \leq L_1$$

$$\frac{y_2(x)}{C_1} = \frac{A_1}{C_1}\,[\psi_5(\psi_1 cos\lambda x + \psi_3 sin\lambda x + sinh\lambda x)) \qquad (5.10)$$

$$+\psi_7\,(\psi_2 cos\lambda x + \psi_4 sin\lambda x + cosh\lambda x)]$$

$$+\,[\psi_6(\psi_1 cos\lambda x + \psi_3 sin\lambda x + sinh\lambda x))$$

$$+\psi_8\,(\psi_2 cos\lambda x + \psi_4 sin\lambda x + cosh\lambda x)]$$

$$L_1 \leq x \leq L$$

The value of $\frac{A_1}{C_1}$ is evaluated using equation (3.28), which shows that

$$\frac{A_1}{C_1} = \frac{-\psi_{10}}{\psi_9}$$

Where ψ_{10} and ψ_0 are function of frequency, and spring constant K. From these equations and utilizing program III which solves the previous equation, Figure 5.5, 5.6, and 5.7 are obtained. These Figures represent the first, second, and third mode, respectively. The output is normalized with respect to the maximum vibration amplitude.

First mode shape was measured by using a transducer, and an accelerometer mounted on the beam, as mentioned before. The accelerometer was kept at the clamped end of the beam to give the input values, while the transducer was moved along the beam to measure the mode amplitude. Plot of the measured, and simulated first mode is shown in Figure 5.8.

5.4 Dynamic Behaviour Of A Cracked Beam

This section focus on the dynamic behaviour of the cracked beam as a function of crack parameters. The vibration amplitude, the slope, and the crack compliance are considered.

5.4.1 Amplitude Behaviour

The vibration mode shape changes as a function of crack location and depth. Equations (5.9) and (5.10) describe the mode shape for cracked beam. These two equation can be written as,

$$\frac{y_1(x)}{C_1} = \frac{A_1}{C_1}(sin\lambda x + \frac{K}{2EI\lambda}(cosh\lambda x - cos\lambda x))+ \qquad (5.11)$$

$$(sinh\lambda x + \frac{K}{2EI\lambda}(cosh\lambda x - cos\lambda x))$$

$$0 \leq x \leq L_1$$

$$\frac{y_2(x)}{C_1} = \frac{A_1}{C_1}\left[\psi_5(\psi_1 cos\lambda x + \psi_3 sin\lambda x + sinh\lambda x)\right. \tag{5.12}$$

$$\left.+\psi_7\left(\psi_2 cos\lambda x + \psi_4 sin\lambda x + cosh\lambda x\right)\right]$$

$$+\left[\psi_6(\psi_1 cos\lambda x + \psi_3 sin\lambda x + sinh\lambda x)\right)$$

$$\left.+\psi_8\left(\psi_2 cos\lambda x + \psi_4 sin\lambda x + cosh\lambda x\right)\right]$$

$$L_1 \leq x \leq L$$

Where $\frac{y_1}{C_1}$ and $\frac{y_2}{C_1}$ give the mode shape, where C_1 and $\frac{A_1}{C_1}$ are constant. The value of $\frac{A_1}{C_1}$ is evaluated using equation (3.28) which states that

$$\frac{A_1}{C_1} = -\frac{\psi_{10}}{\psi_9}$$

In these equations ψ_9 and ψ_{10} are function of spring constant K, frequency, and crack parameters. Fig. 5.9 represent the first mode for a cracked beam at a distant of 3cm and depth of 7mm from the clamped end. Program III is utilized to get these Figures. This program was developed utilizing equations (5.11) and (5.12). The output was normalized with respect to the maximum vibration amplitude. Plots of the measured, and simulated first mode, for the same beam is shown in Figure 5 .10. In this Figure the measured value is for a beam with slot at a distant 3cm and depth of 7mm from the clamped end. It is noticed from these Figures the amplitude is effected by the crack, and this effect is characterized by the crack depth. This effect will be discussed in a later sections thoroughly.

5.4.2 Slope Behaviour

Equation (5.11) and equation (5.12) are derived with respect to x to obtain the following slope equations

$$\frac{1}{C_1}\frac{dy_1}{dx} = \frac{A_1}{C_1}(\lambda cos\lambda x + \frac{K}{2EI\lambda}(\lambda sinh\lambda x + \lambda sin\lambda x)) + \tag{5.13}$$

$$(\lambda cosh\lambda x + \frac{K}{2EI\lambda}(\lambda sinh\lambda x + \lambda sin\lambda x))$$

$$0 \leq x \leq L_1$$

$$\frac{1}{C_1}\frac{dy_2}{dx} = \frac{A_1}{C_1}[\psi_5(-\psi_1\lambda sin\lambda x + \psi_3\lambda cos\lambda x + \lambda cosh\lambda x)) \tag{5.14}$$

$$+\psi_7(-\psi_2\lambda sin\lambda x + \psi_4\lambda cos\lambda x + \lambda sinh\lambda x)]$$

$$+[\psi_6(-\psi_1\lambda sin\lambda x + \psi_3\lambda cos\lambda x + \lambda cosh\lambda x))$$

$$+\psi_8(-\psi_2\lambda sin\lambda x + \psi_4\lambda cos\lambda x + \lambda sinh\lambda x)]$$

$$L_1 \leq x \leq L$$

Figure 5.11 shows the slope at first mode, for a cracked beam at a distant of 3cm and depth of 7mm from the clamped end, a jump is noticed at the crack location. This jump depends on the moment value at the crack location according to the following boundary condition.

$$y_1\prime(L_1) + \frac{EI}{K_T}y_1\prime\prime(L_1) = y_2\prime(L_1)$$

Program IV produces the data for Figure 5.11

5.4.3 Compliance Behaviour

The crack compliance depends on the crack orientation and magnitude with respect to the main dimensions of the cracked member. It also depends on the applied loadings and the mode of deformation, as mentioned in Chapter 2, and 3.

Fig. 10.12 represents the compliance versus the crack depth utilizing program V, this program was made to get the value of compliance according to Dimarogonas

equation. The bending spring which represents the crack effect $K_T = \frac{1}{c}$ as mentioned before is represented by Fig. 10.13 versus the crack depth, each of these Figures at first mode.

5.5 Crack Identification

This section focuses on utilization the experimental data for the identification of the crack parameters. First, the crack depth at a known location is considered and second, the general case of finding the crack location and depth is dealt with.

5.5.1 Crack Depth Evaluation At Known Location

Theoretically, it is possible to know the depth of the crack if its location is known. This is done by knowing the values of frequency for a certain specimen at the first mode. Equation (3.29) could be solved using the Bisection method for the crack depth if the crack location is known. This evaluation is done using program VI.

Table (5.7) and (5.8) give the estimated slot depths for known locations for different specimens.

From Table (5.7) it is obvious that the accuracy in slot depth determination increases directly with the slot depth. This is shown clearly in Fig. (5.14) which shows the relation between the error in depth determination and the magnitude of depth of the slot.

Table (5.8) shows that the closer the location of the slot to clamped end, the more the accuracy in the estimated slot depth. This is so because the reduction caused by the slot closer to clamped end is greater than that caused by the slot which is remote from the clamped end at the same depth. This behaviour is shown in Figure 5.15.

The exact crack depth was found by dipping the specimen in liquid Nitrogen up to the crack location to make the beam brittle. By fracturing the treated beam at the crack location the depth of the crack was measured. This procedure was done

only for two specimens due to technical complications. It should be mentioned that the propagation of crack in these two specimens was non-uniform. Consequently, the average of the irregular depth was evaluated and this average was considered as the theoretical depth. Table (5.9) gives the estimated depths for different cracks at various location. The photos 1, and 2 show the specimens that were dipped in liquid Nitrogen.

From the above it is proved that the crack can be determined provided its location and the frequency of the specimen at the first mode only.

Table 5.7: Exact and estimated depths for slots at 3cm from the fixed end.

Slot depth mm	Estimated slot depth mm	Error in Est.
1	0.788	21.2%
3	2.3642	21.19%
5	4.6696	6.6%
7	6.66097	4.8%
8	7.66898	4.1%

Table 5.8: Estimated depths at different location for a slot with 3mm exact depth.

Slot location cm	Slot Depth Est.	Error
1	2.6176	12.74%
2	2.59933	13.35%
3	2.3642	21.19%
4	2.38369	20.54%
5	2.26858	24.38%
6	2.33	22.33%
7	2.28408	23.86%
8	1.917	36.1%

Table 5.9: Crack Estimation at different locations and different depths

Crack location cm	Crack Depth	crack depth Est.	Error
1	2.75	2.173389	20.967%
3	2.5	1.7678794	29.2848%
5	—	1.588699	—%
6	—	2.0638542	—%

5.5.2 Identification of crack or slot location and magnitude

From the previous discussion it is obvious that if the crack or the slot location is determined it will be possible to evaluate its depth.

In this section a method for determining the crack location will be described. It is shown that the slot or the crack will cause an inflection in the first mode shape at the same spot where the crack or the slot is located. The part of the specimen that follows the inflection-point tends to be straight. It becomes more straight the depth of the crack increases. This inflection produces a sharp edge as shown in Figures 5.16, 5.17, 5.18, 5.19, where these Figures show the mode shapes for different crack depth at a constant location. The sharpness of this edge increases as the depth of the crack or the slot increases. It is possible to recognize this inflection point, and its recognition becomes easier when the depth becomes significantly large.

This is due to the compliance which increases directly with the crack depth. The increase in the compliance leads to a condition in which the part that follows the crack or the slot move more freely as one bulk mass.

The crack or the slot location determination depends on the accuracy of the instrumentation used in detection the amplitude along the specimen. The instrument used for this purpose in this study especially the Magnetic Transducer were not sat-

isfactory in determining the inflection point. For instance, the Magnetic Transducer is effected by the magnetic field in the exciter. In addition, the points at which the amplitude values were obtained were not closed enough, which made it difficult to determine the required inflection point accurately.

To support this study with other experimental results, the result obtained by Rizos, et al.[13] are examined in the following. Rizos, et al. results are shown in Figure 5.20 where the first mode shape of a cracked beam is plotted. The inflection point is clearly located at a distance of 140 mm experimentally and theoretically. Consequently, the crack location for this specimen is determined.

And since the crack location is determined, the depth can be evaluated easily following the same previously mentioned method.

It is concluded in this study that the inflection point must be determined to locate the crack location. i.e the amplitude values for the first mode should be taken along the specimen to determine the inflection point.

Rizos et al. [13] had mentioned that measuring the amplitudes at two arbitrary points in a particular sample, is enough to locate the crack and its depth.

There is a defect in Rizos, et al. method in determining the crack location. Since the two readings are taken arbitrary, there are three possibilities, the first is to read the two points in locations before the crack, the second is to read the two points in locations after the crack, and the third is to read one point before and one point after the crack. In the first and second possibilities the readings do not give accurate representation of the cracked beam mode shape because the two points behaviour is governed by the same function either y_1 or y_2 as shown in Figure 5.21.

The third possibility is hard to guarantee. Since choosing points before and after the crack requiring a previous knowledge about the location of the crack. In addition

different depth location combination may give the same amplitude readings. Such a case is shown in Figure 5.22

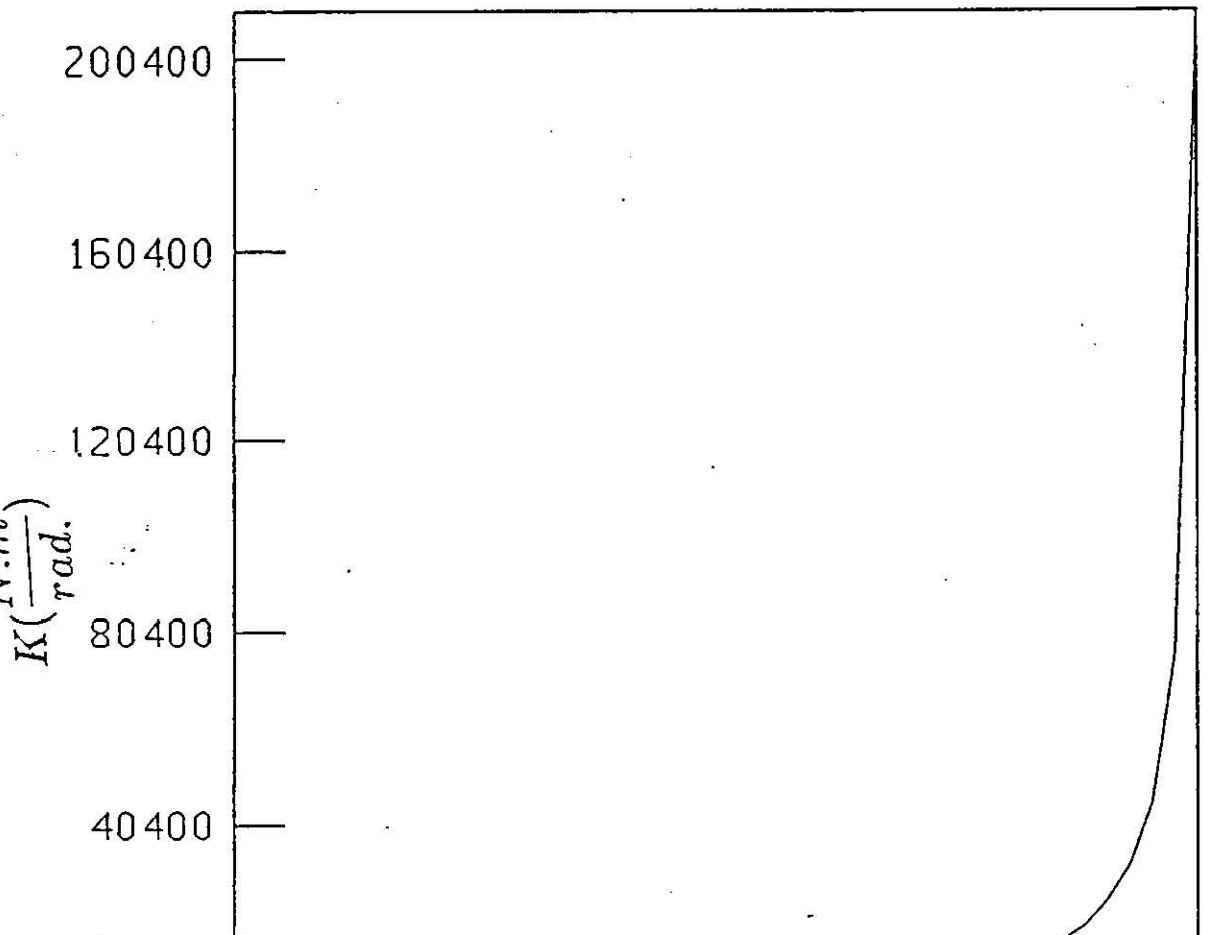

Figure 5.2: Spring constant at the clamped end Vs. the frequency of the first mode.

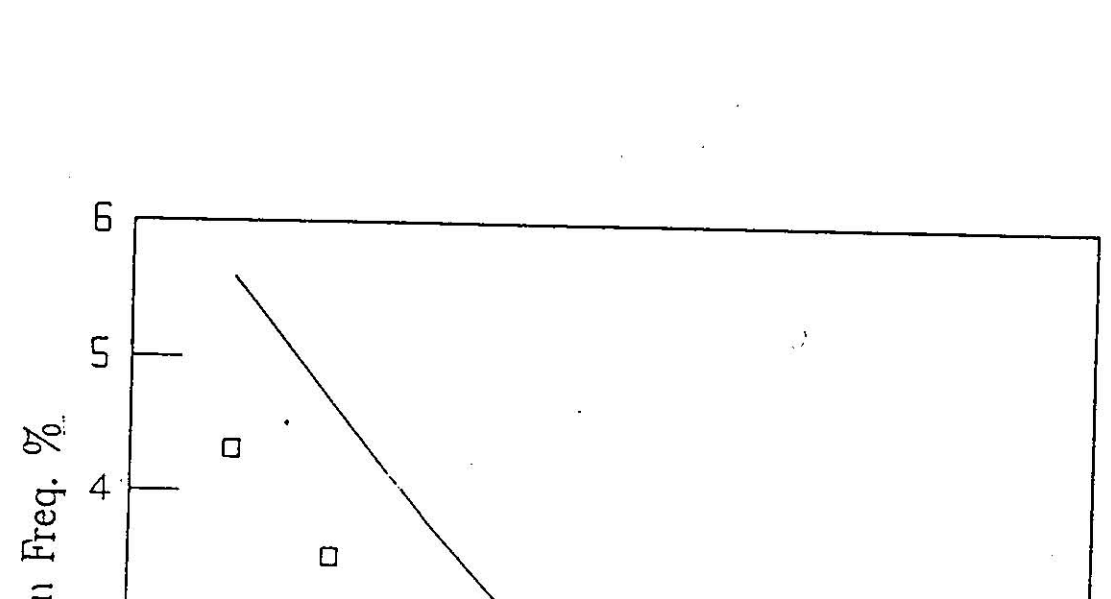

Figure 5.4: Relation between the reduction in frequencies, at first mode for cracks at different locations and constant depth 3mm. Where (—) is the theoretical values and (o) is the experimental values.

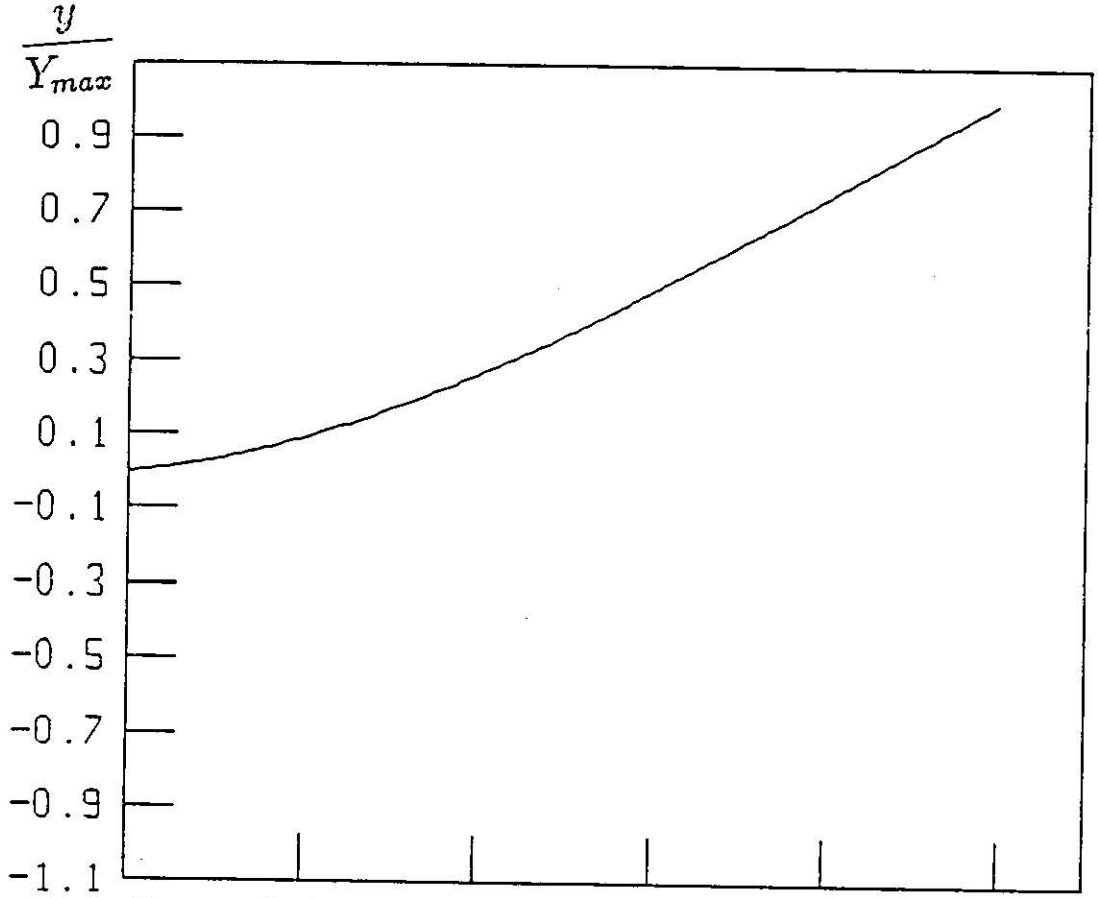

Figure 5.5: First mode shape, theoretically at 275 Hz for uncracked specimen.

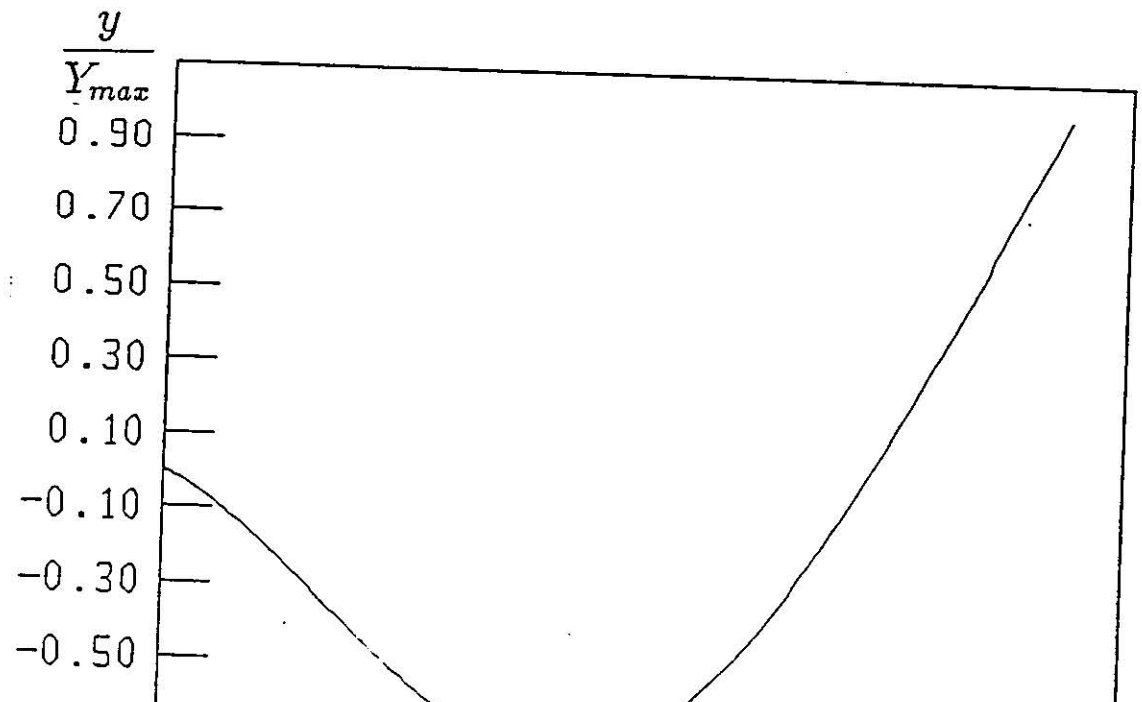

Figure 5.6: Second mode shape, theoretically for uncracked specimen.

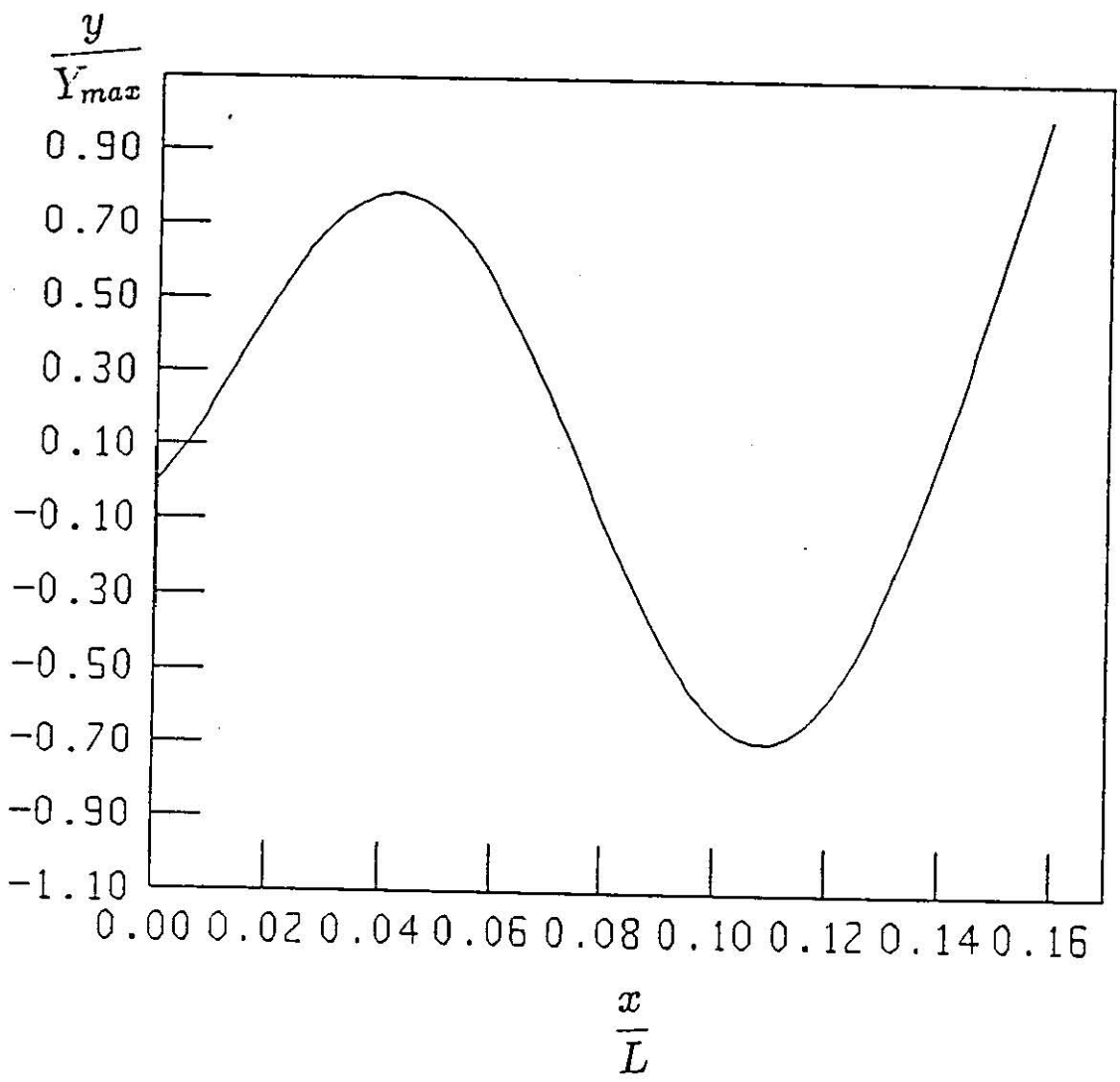

Figure 5.7: Third mode shape, theoretically for uncracked beam.

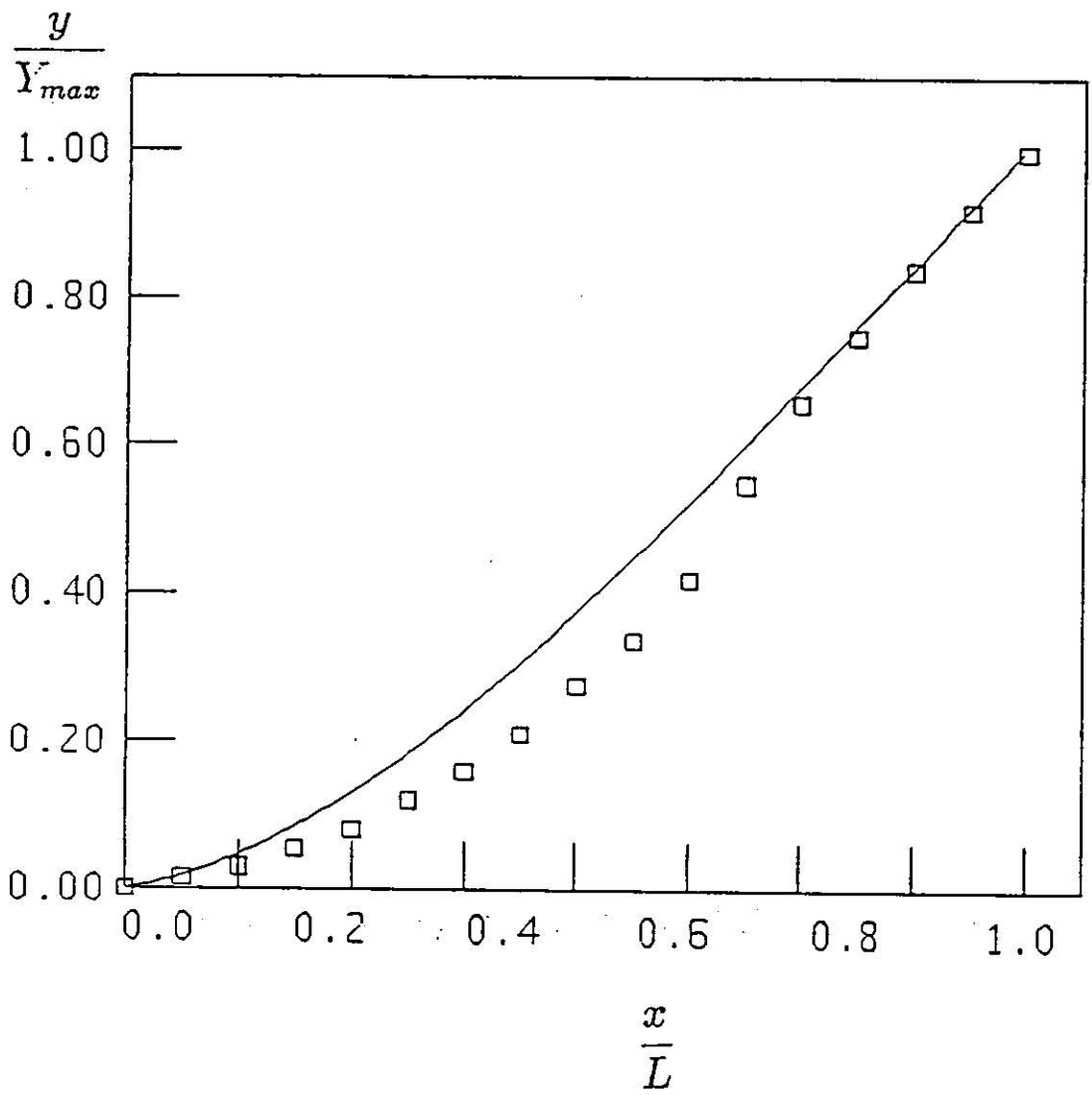

Figure 5.8: First mode shape experimentally and theoretically for uncracked beam. Where (—) is the theoretical values and (o) is the experimental values.

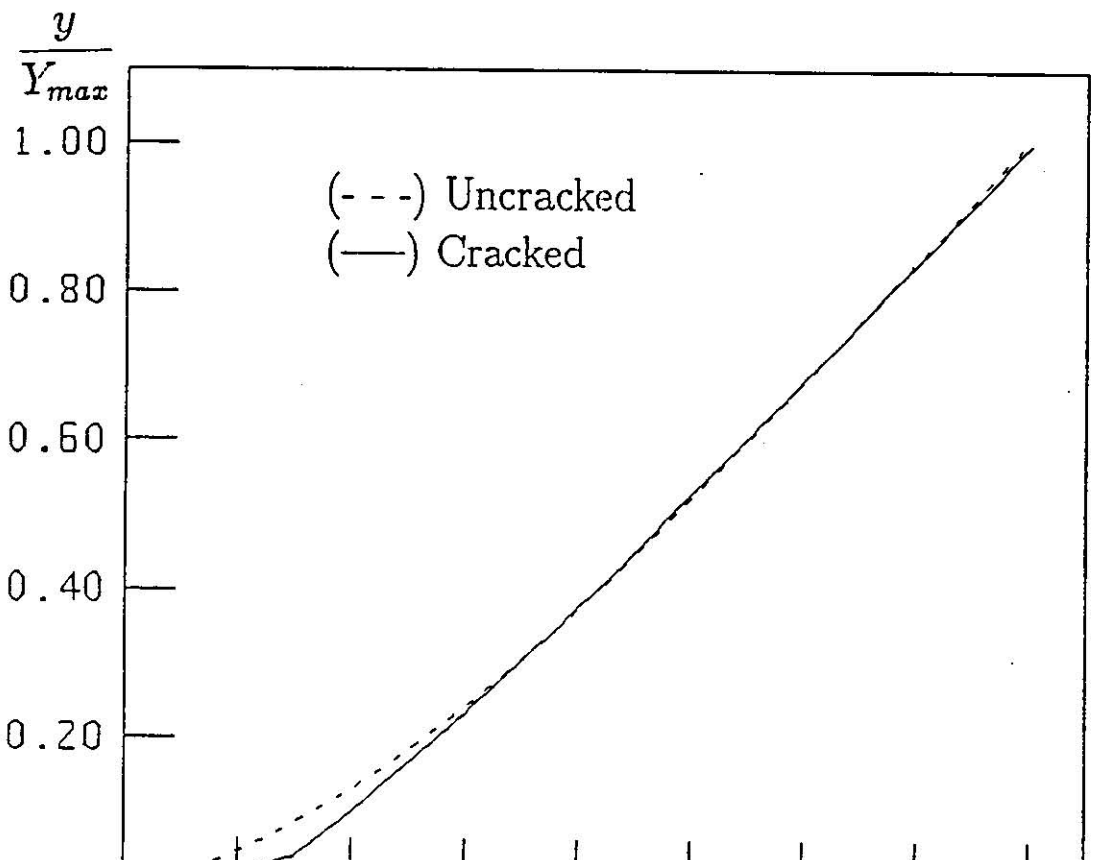

Figure 5.9: First mode shape for cracked beam at 3cm position and at a depth of 7mm. Where (- - -) is the values of uncracked beam, and (—) is the values of crack beam.

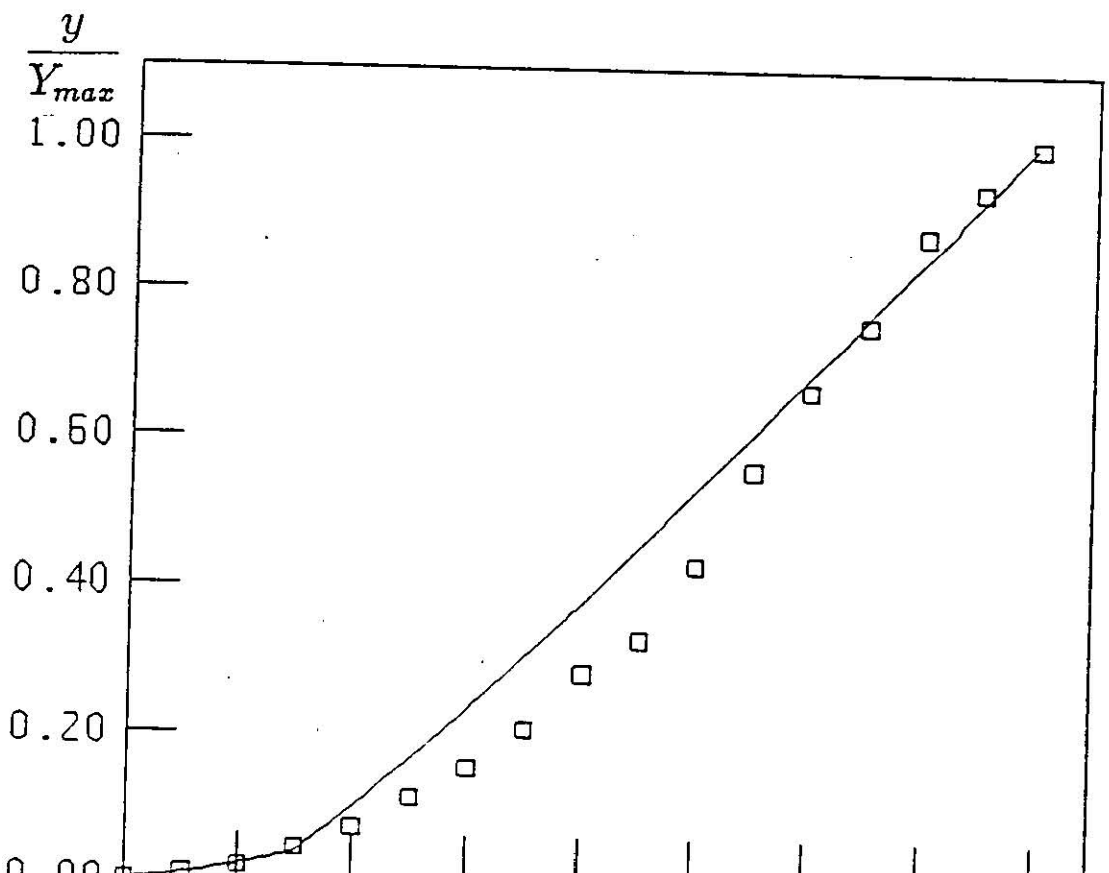

Figure 5.10: Theoretical (- - -) and measured (0) first mode shape for specimen with crack at 3cm location and at depth 7mm.

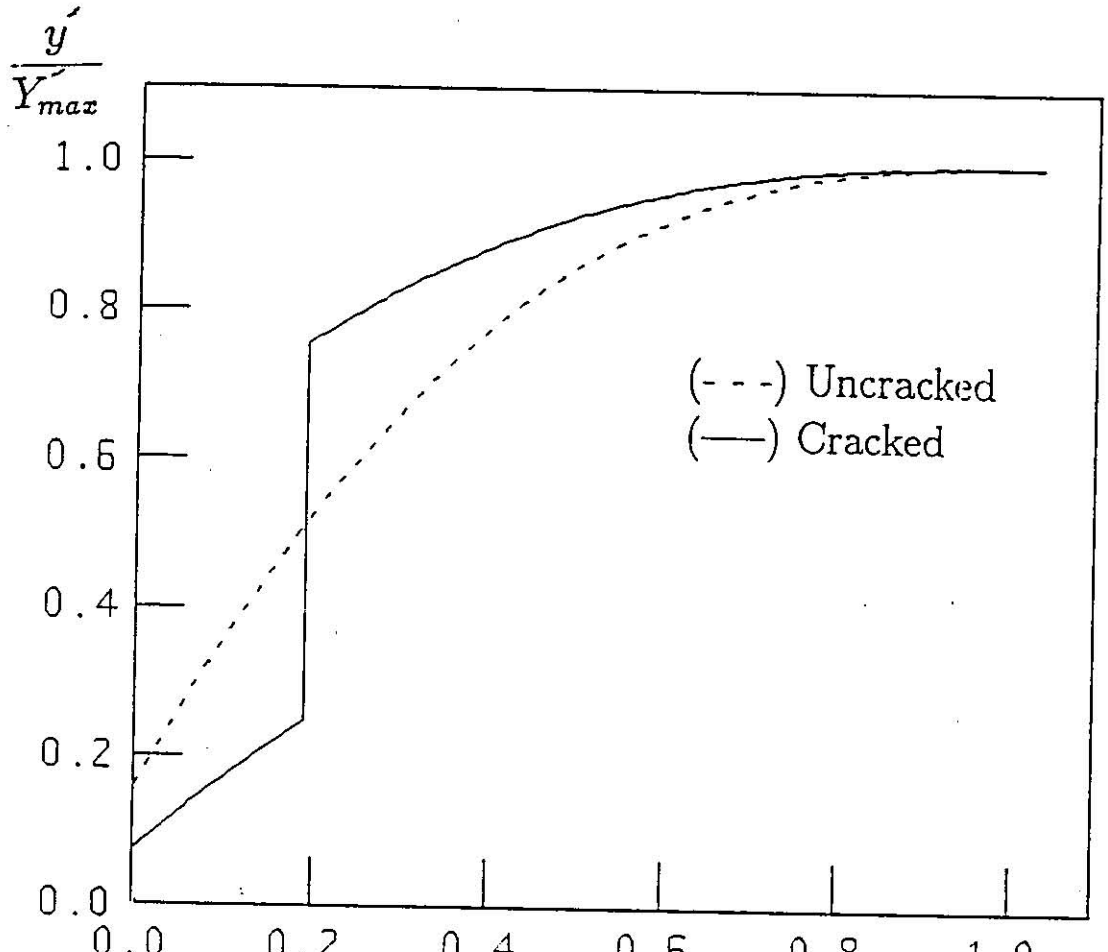

Figure 5.11: The slope over specimen, at the first mode. Where (- - -) is the values of uncracked beam, and (—) is the values of cracked beam at location of 3cm and at the depth of 7mm

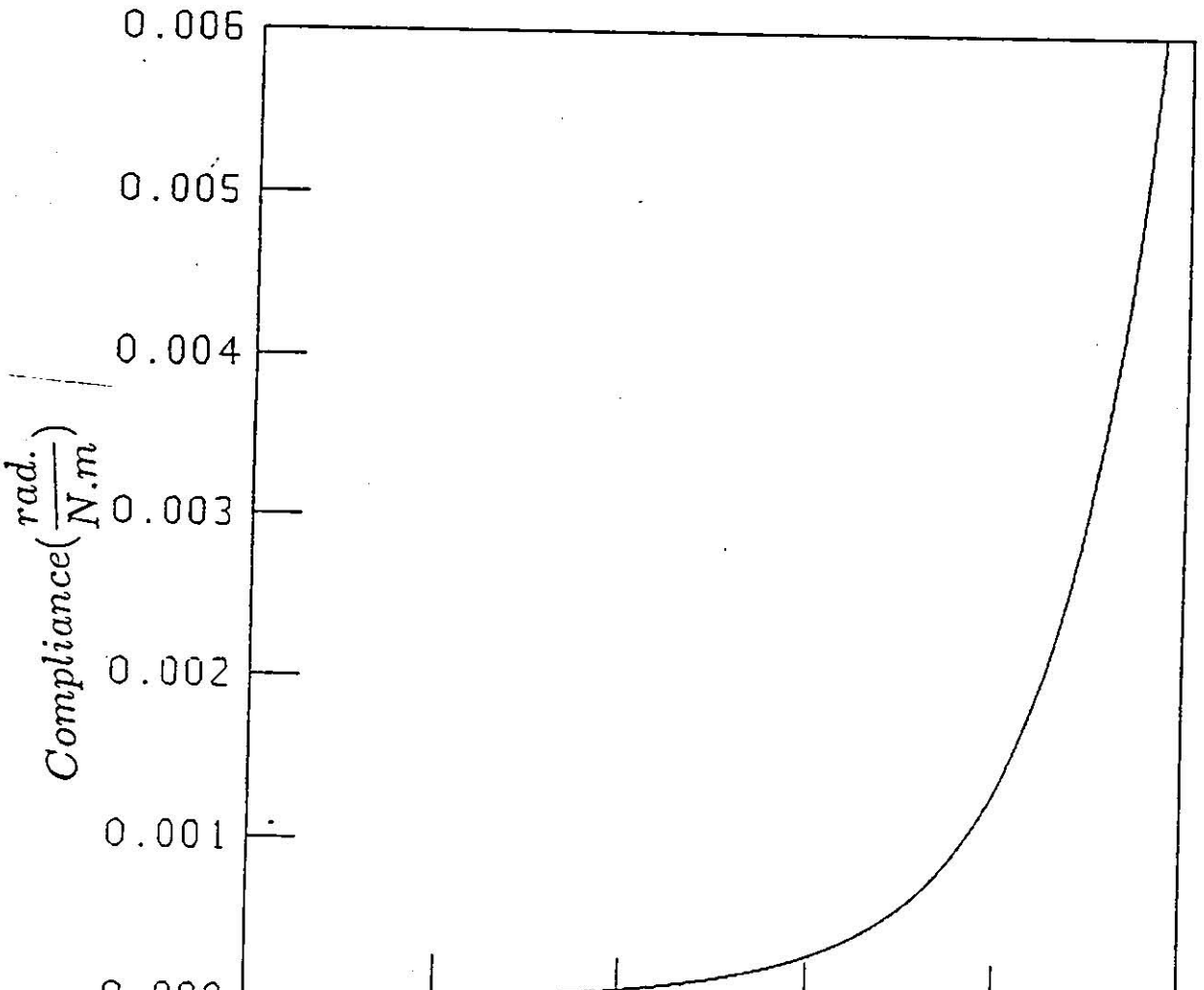

Figure 5.12: Compliance at the crack location Vs. the crack depth.

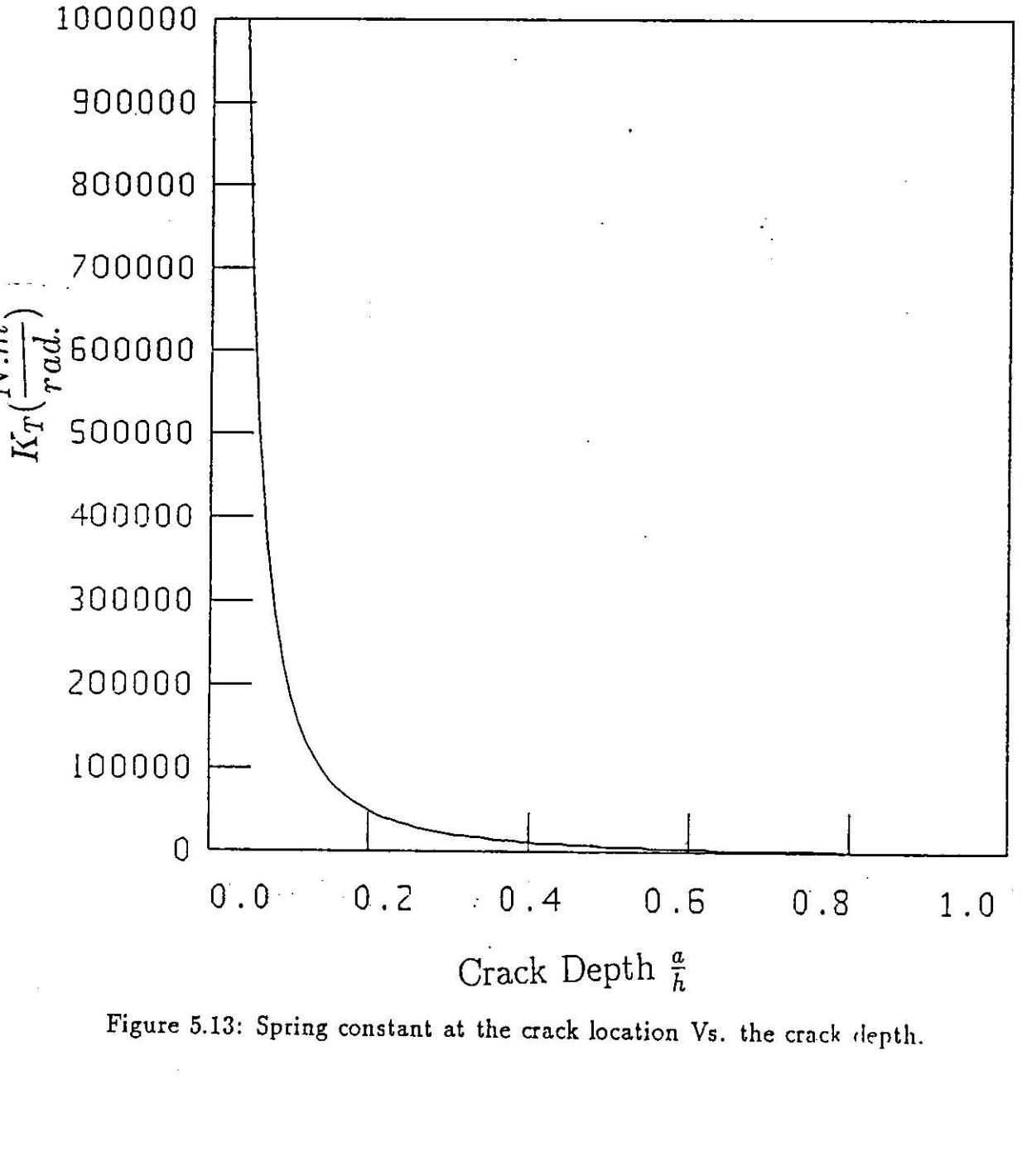

Figure 5.13: Spring constant at the crack location Vs. the crack depth.

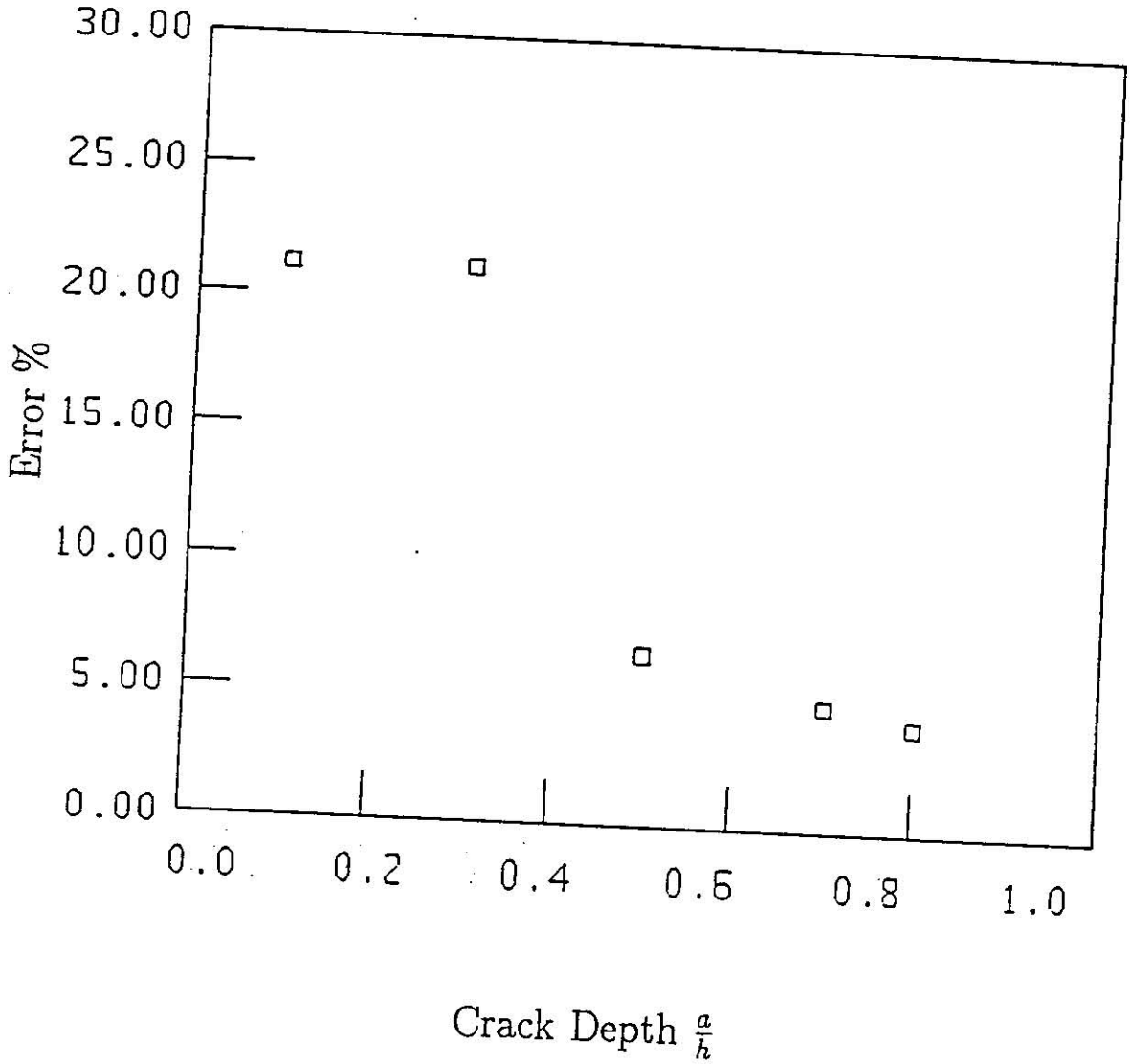

Figure 5.14: Error in crack depth evaluation Vs. the crack depth at 3cm location, utilizing the experimental natural frequency of the first mode.

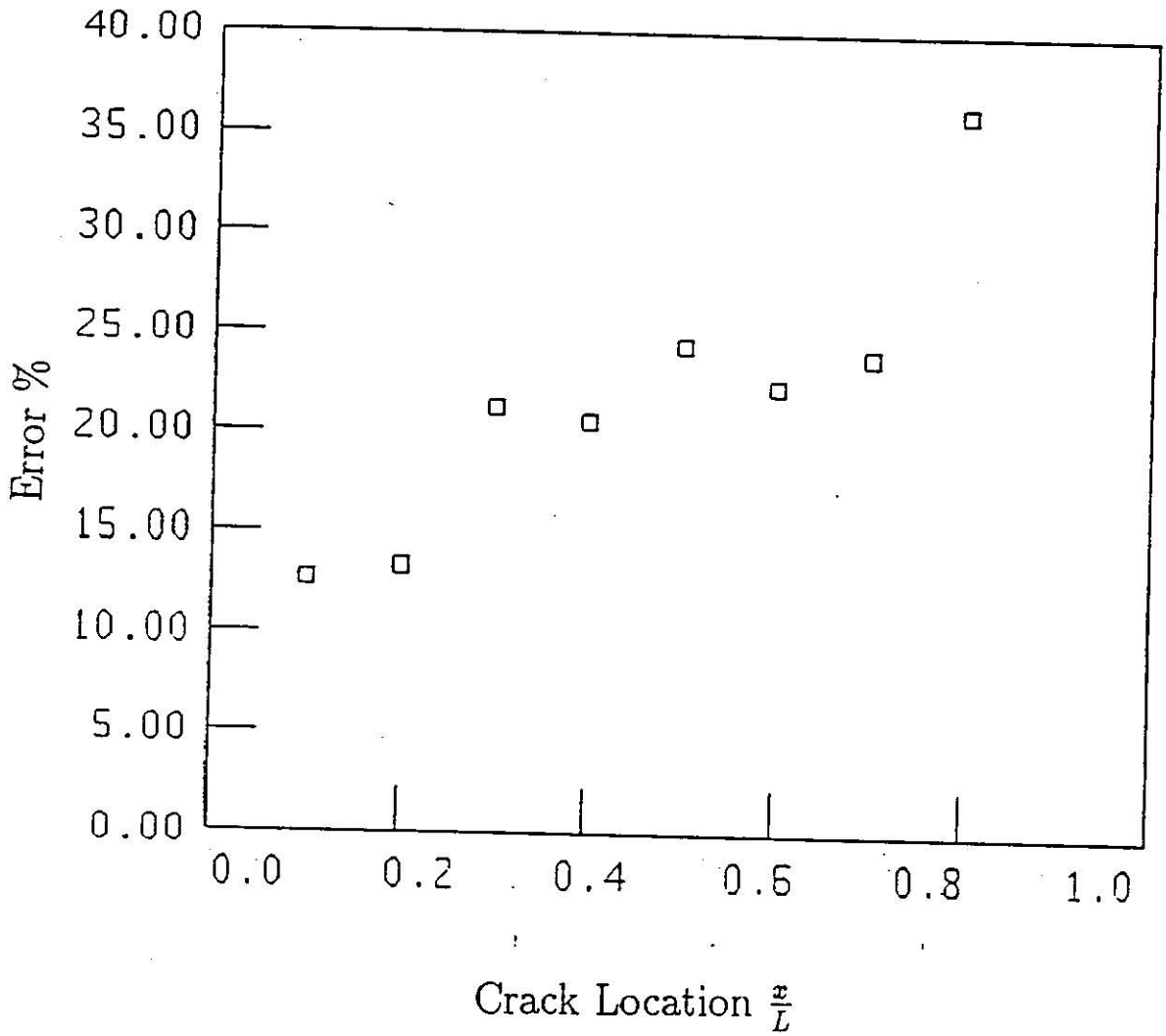

Figure 5.15: Error in crack depth evaluation Vs. crack location at constant crack depth 3mm. Utilizing the experimental natural frequency of the first mode.

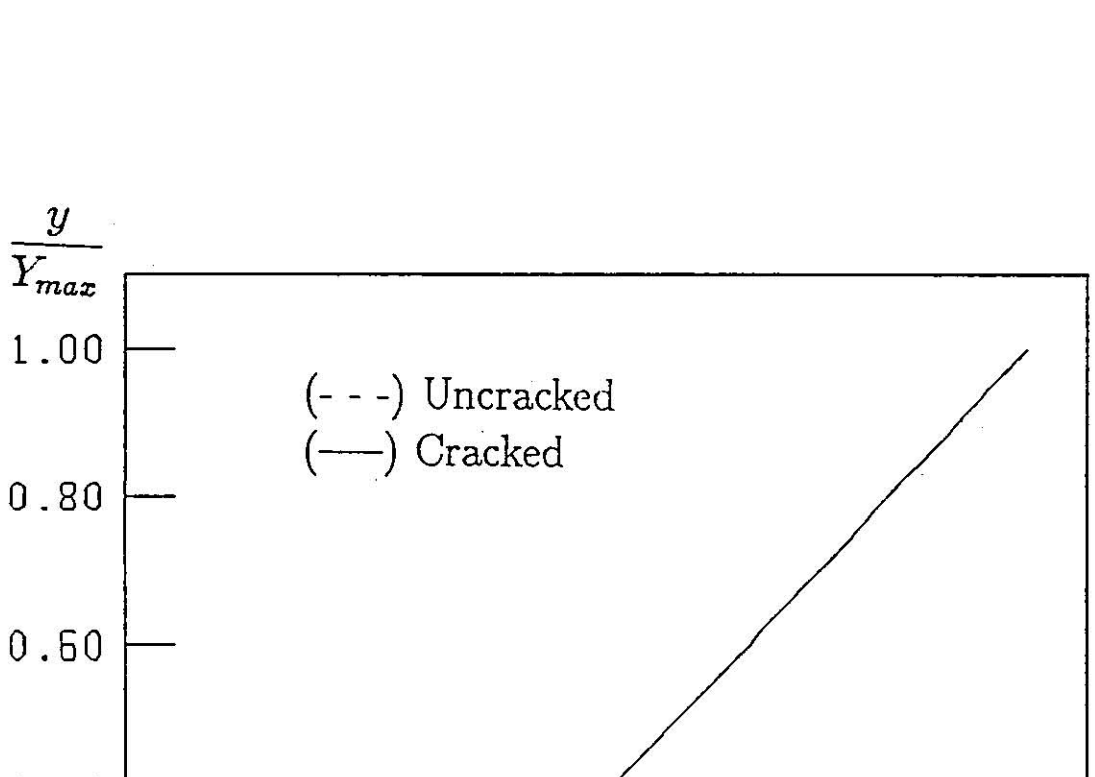

Figure 5.16: Cracked beam at 4cm location and 3mm depth. Where (- - -) is the values of uncracked beam, and (—) is the values of cracked beam.

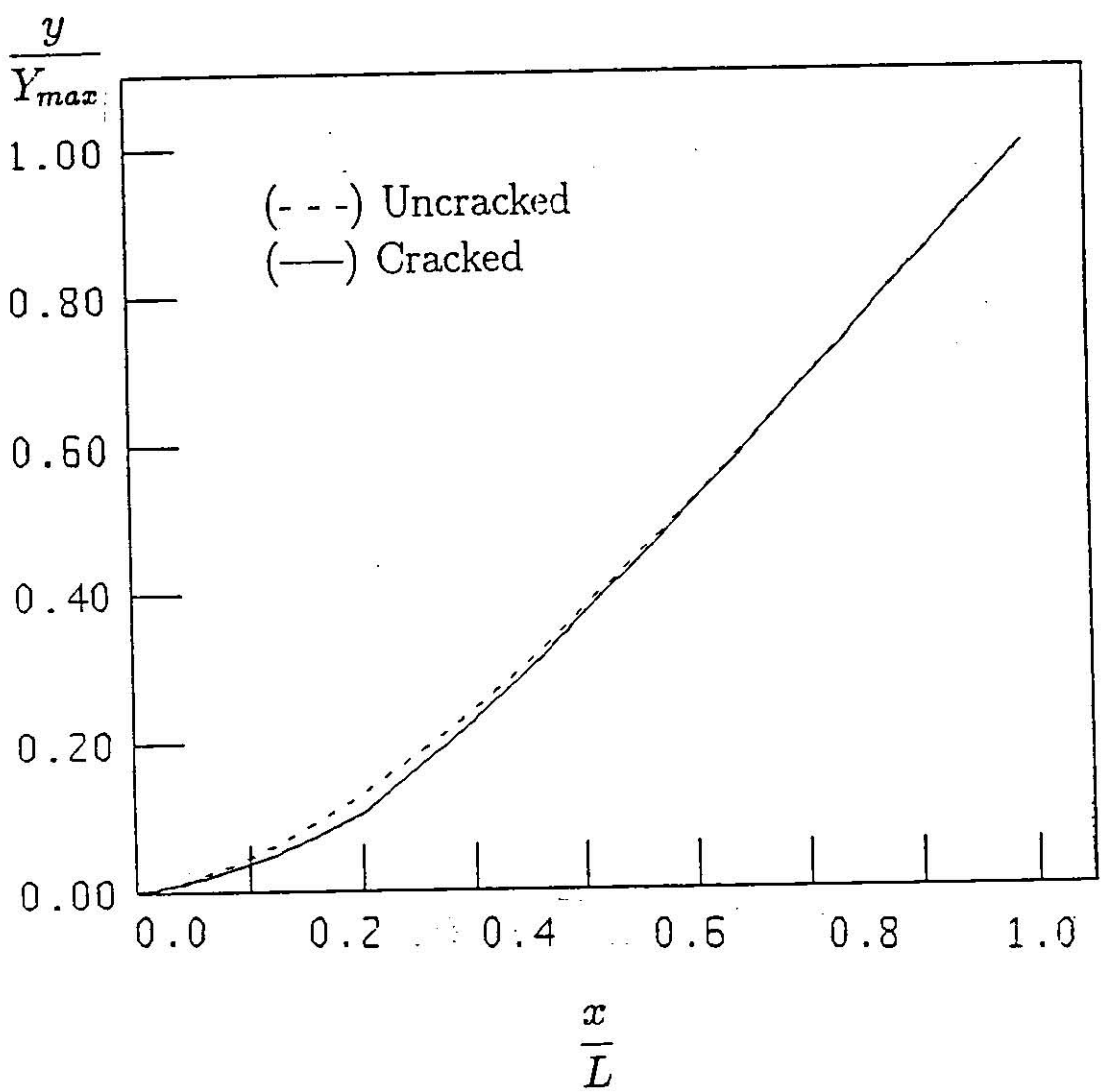

Figure 5.17: Cracked beam at 4cm location and 5mm depth. Where (- - -) is the values of uncracked beam, and (—) is the values of cracked beam.

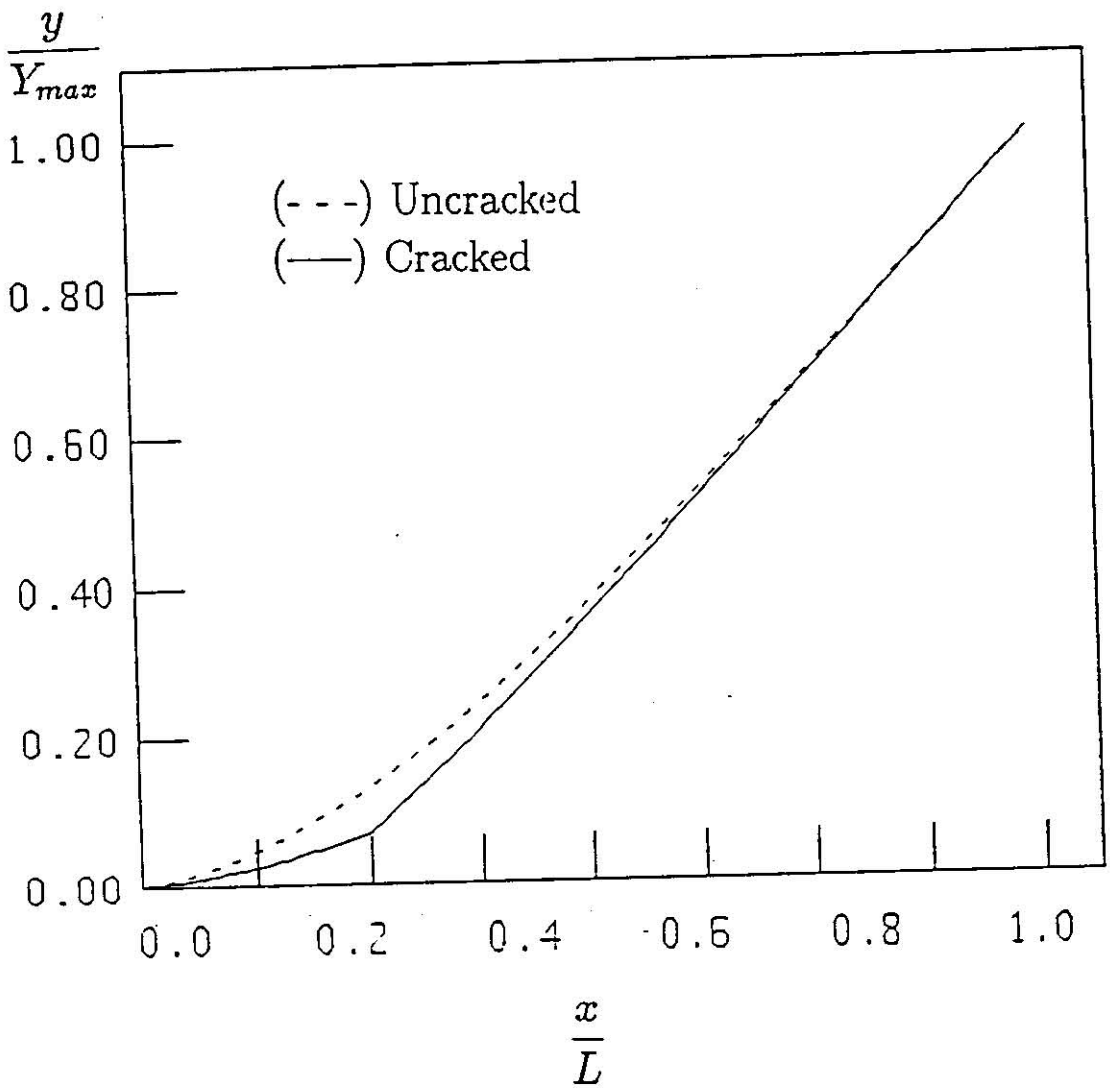

Figure 5.18: Cracked beam at 4cm location and 7mm depth. Where (· - -) is the values of uncracked beam, and (—) is the values of cracked beam.

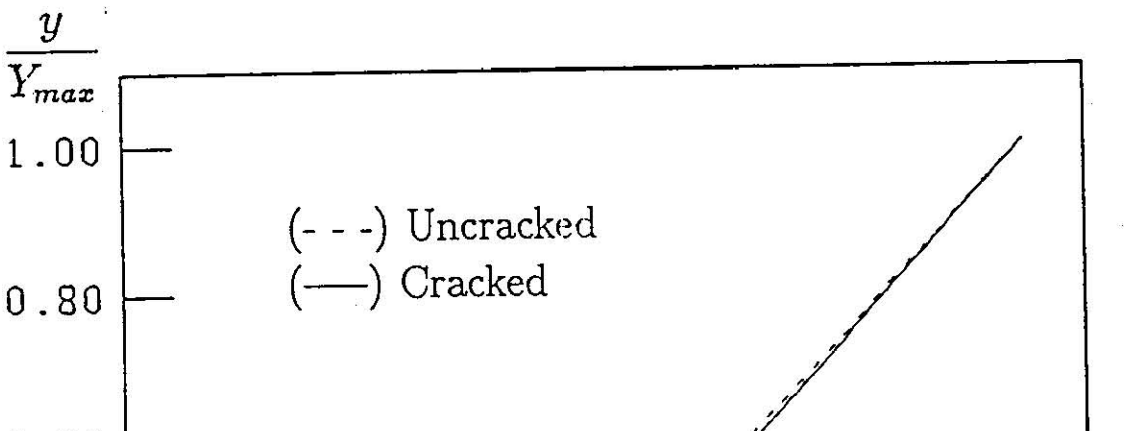

Figure 5.19: Cracked beam at 4cm location and 4mm depth. Where (- - -) is the values of uncracked beam, and (—) is the values of cracked beam.

Figure 5.20: The first mode shape as stated by Rizos et al. [13].

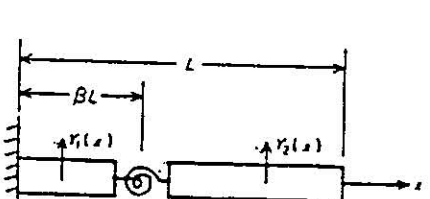

Figure 5.21: Cracked cantilever beam model as stated by Rizos et al.[13].

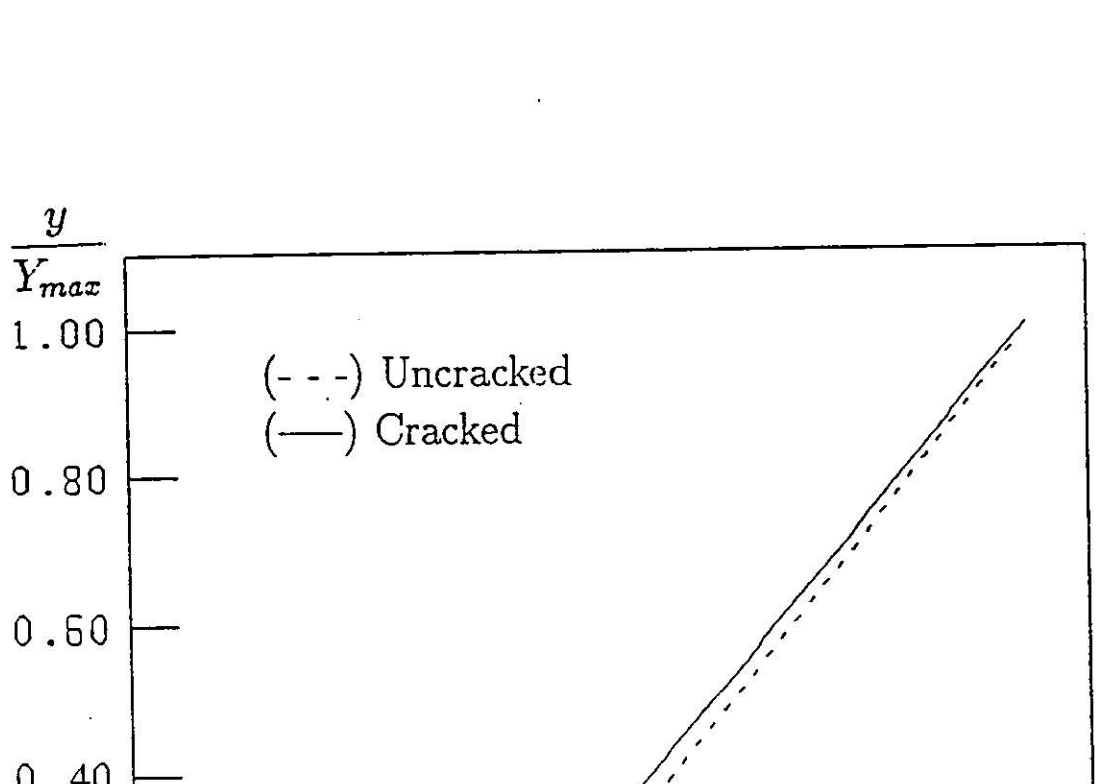

Figure 5.22: Cracked beam at 7cm location and 7mm depth which represented by (—),and cracked beam at 8cm and 7.51344 depth which represented by (- - -).

Chapter 6

CONCLUSION AND RECOMMENDATIONS

6.1 Conclusions

The following set of results and conclusions are reached in this study.

1. It was found that in the case of knowing the exact location of the crack it would be easy to compute the crack depth taking into consideration the value of the natural frequency of the first mode.

2. It is possible to identify the crack location by locating the inflection point that appears in the amplitude of the first mode where the two have the same location. And the deeper the crack is, the easier to identify the inflection point.

3. The accuracy of crack estimation increases with the crack depth and with the closeness of the crack to the clamped end.

4. Crack tends to reduce the natural frequency of the first mode, and this reduction is directly proportional to the crack depth and inversely proportional to the crack distance from the clamped end.

5. Using the first mode to locate the crack and its depth was quite satisfactory. Since the effect of the crack on the first mode was very detectable. In addition, higher modes frequencies and shapes are difficult to detect due to instrument limitations.

6.2 Recommendations

For further work on this topic, the following issues are proposed.

1. The instruments accuracy was questionable specially the magnetic Transducer. Future study should use more reliable instruments.

2. In this research the equation of Dimarogonas study which had dealt with the bending spring to represent the crack was employed. It is recommended strongly to make more studies in Dimarogonas correlations to establish their reliability.

3. This and similar studies must be performed on other mechanical elements so that a general procedure could be established for vibrational techniques in crack detection.

REFERENCES

1. Chondros, T.G. and Dimarogonas, A.D. " Identification of cracks in welded joints of complex structures", Journal of Sound and Vibration, v. 71, 1980 , pp. 121-125.

2. Dimargonas, A.D. "Vibration Engineering", St. Paul, Mennesota: west Publishers, 1976.

3. Dimargonas, A.D. and Paipeties, S.A. " Analytical Methods in Rotor Dynamics", London: Elsvier Applied science, 1983.

4. Andantis, P., Aspragations, N., and Dimarogonas, A.D. "Diagnosis of cracks on concrete frames due to earth quakes by vibration response analysis", J. of Sound and vibration, v. 102, 1983, pp. 17-21.

5. Kirshmer, P.G. " The effect of discontinuities on the natural frequency of beams", Proceeding of the American Society of testing and Materials, v. 44, 1944, pp. 897-904.

6. Thomson, W.J. " Vibration of slender bars with discontinuities in stiffness", Journal of Applied Mechanics, v. 17, 1943, pp. 203-207.

7. Petroski, H.J. " Simple static and dynamic models for the cracked elastic beam", International Journey of Fracture, v. 17, 1981, pp. 71-76.

8. Petroski, H.J " Structural dynamics of piping with stable cracks: some simple models", International Journal of Pressure Vessel and Piping, v. 13, 1983, pp. 1-18.

9. Grabowski, B. " The vibrational behaviour of a rotor containing a transverse crack", Journal of Mechanical Design, v. 102, 1979, pp. 140-146.

10. Inagaki, T., Kanki, H., and Shiraki, K. " Transverse vibrations of a general cracked-rotor bearing system", Journal of Mechanical Design, v. 104, 1981, p. 11.

11. Christides, S., and Barr, A.D "One-dimensional theory of cracked Bernoulli-Euler beam", ASME, v. 111, 1984, pp. 81-84.

12. Rajab, M.D., and Al-Sabeeh, A. " Vibrational Characteristics of Cracked Shaft", Journal of Sound and Vibration, v. 147, no. 3, 1991, pp. 465-473.

13. Rizos, P.F, Aspragathos, N., and Dimarogonas, A.D " Identification of crack location and magnitude in a cantilever beam from the vibration modes", J. of Sound and vibration, v. 138, no. 3, 1990, pp. 381-388.

14. Cawely, P. " Non-destructive testing of mass produced components by natural frequency measurements", Proc. I. Mech. Eng., v. 199, no. 3, 1985, pp. 161-168.

15. Caweley, P., and Ray, R. " Acomparison of the Natural Frequency Changes Produced by Cracks and Slots", J. of Vibration, Acoustics, Stress, and Reliability in Design, vol. 110, 1988, pp. 366-370.

16. Ismail, F., Ibrahim, A., and Martin, H. " Identification of fatigue cracks from vibration testing",J. of Sound and vibration v. 140(2), 1990, pp. 305-317.

Appendix A

APPENDIX A

Table A.1 : Experimental first mode shape at 275 Hz for uncracked beam

Position(cm)	V.(r.m.s) mv	V.norm.
0	1.7	0
1	1.78	0.015
2	1.86	0.029
3	1.99	0.053
4	2.13	0.079
5	2.35	0.119
6	2.56	0.158
7	2.84	0.21
8	3.2	0.276
9	3.53	0.337
10	3.98	0.42
11	4.68	0.549
12	5.28	0.659
13	5.77	0.749
14	6.26	0.84
15	6.7	0.921
16	7.13	1

Table A.3 : Experimental first mode shape at 268.5 Hz for a beam with slot at 3cm position and 3mm depth.

Position(cm)	V.(r.m.s) mv	V.norm.
0	1.68	0
1	1.75	0.0128
2	1.82	0.0256
3	1.95	0.0494
4	2.11	0.0786
5	2.32	0.117
6	2.57	0.16
7	2.84	0.212
8	3.21	0.28
9	3.53	0.338
10	3.98	0.42
11	4.66	0.545
12	5.3	0.662
13	5.79	0.751
14	6.31	0.846
15	6.73	0.923
16	7.15	1

Table A.4 : Experimental first mode shape at 247.3 Hz for a beam with slot at 3cm position and 5mm depth.

Position(cm)	V.(r.m.s) mv	V.norm.
0	2.13	0
1	2.21	0.012
2	2.29	0.024
3	2.45	0.048
4	2.64	0.0766
5	2.91	0.117
6	3.19	0.1592
7	3.55	0.2132
8	4.33	0.285
9	4.03	0.3303
10	5.00	0.4309
11	5.86	0.5601
12	6.59	0.6697
13	7.19	0.7597
14	7.94	0.8724
15	8.41	0.9429
16	8.79	1

Table A.5 : Experimental first mode shape at 202.7 Hz for beam with slot at 3cm position and 7mm depth.

Position(cm)	V.(r.m.s) mv	V.norm.
0	2.00	0
1	2.07	0.0104
2	2.14	0.0208
3	2.31	0.046
4	2.50	0.0743
5	2.77	0.1144
6	3.05	0.156
7	3.41	0.2095
8	3.92	0.2853
9	4.23	0.3313
10	4.91	0.4324
11	5.78	0.5616
12	6.51	0.6701
13	7.11	0.7593
14	7.93	0.8811
15	8.33	0.9405
16	8.73	1

Table A.6 : Experimental first mode shape at 167.3 Hz for a beam with slot at 3cm position and 8mm depth.

Position(cm)	V.(r.m.s) mv	V.norm.
0	2.10	0
1	2.17	0.0103
2	2.14	0.0206
3	2.40	0.044
4	2.59	0.0719
5	2.86	0.1116
6	3.14	0.1527
7	3.44	0.1967
8	4.01	0.28505
9	4.36	0.3318
10	5.05	0.4332
11	5.93	0.5624
12	6.67	0.6711
13	7.34	0.7695
14	8.15	0.8884
15	8.53	0.9442
16	8.91	1

Table A.7 : Experimental first mode shape at 263.1Hz for a beam with slot at 1cm position and 3mm depth.

Position(cm)	V.(r.m.s) mv	V.norm.
0	1.95	0
1	2.02	0.0104
2	2.09	0.0208
3	2.29	0.0507
4	2.44	0.0731
5	2.75	0.1194
6	3.02	0.1597
7	3.42	0.2194
8	3.83	0.2806
9	4.23	0.3403
10	4.83	0.4298
11	5.65	0.552
12	6.38	0.6612
13	6.99	0.752
14	7.59	0.842
15	8.12	0.921
16	8.65	1

Table A.8 : Experimental first mode shape at 265.3 Hz for a beam with slot at 2cm position and 3mm depth.

Position(cm)	V.(r.m.s) mv	V.norm.
0	1.98	0
1	2.05	0.0105
2	2.12	0.021
3	2.31	0.0496
4	2.45	0.0707
5	2.76	0.1173
6	3.04	0.1594
7	3.44	0.2195
8	3.91	0.2902
9	4.31	0.3504
10	4.84	0.4301
11	5.65	0.5518
12	6.38	0.6616
13	6.99	0.7534
14	7.57	0.8406
15	8.1	0.9203
16	8.63	1

Table A.9 : Experimental first mode shape at 269.8 Hz for a beam with slot at 4cm position and 3mm depth.

Position(cm)	V.(r.m.s) mv	V.norm.
0	2.00	0
1	2.07	0.0105
2	2.14	0.021
3	2.32	0.0481
4	2.49	0.0737
5	2.73	0.1097
6	2.99	0.1488
7	3.33	0.2000
8	3.79	0.2692
9	4.23	0.3353
10	4.86	0.4301
11	5.72	0.5594
12	6.40	0.6616
13	7.00	0.7518
14	7.65	0.8496
15	8.15	0.9248
16	8.65	1

Table A.10 : Experimental first mode shape at 271.4Hz for a beam with slot at 5cm position and 3mm depth.

Position(cm)	V.(r.m.s) mv	V.norm.
0	1.95	0
1	2.02	0.0105
2	2.09	0.021
3	2.26	0.0466
4	2.42	0.0706
5	2.62	0.1007
6	2.88	0.1398
7	3.28	0.21
8	3.81	0.2796
9	4.18	0.3353
10	4.74	0.4195
11	5.59	0.5473
12	6.32	0.6571
13	6.92	0.7474
14	7.54	0.8406
15	8.07	0.9203
16	8.6	1

Table A.11 : Experimental first mode shape at 272.2 Hz for a beam with slot at 6cm position and 3mm depth.

Position(cm)	V.(r.m.s) mv	V.norm.
0	2.00	0
1	2.06	0.009
2	2.12	0.018
3	2.32	0.0482
4	2.48	0.0723
5	2.59	0.0888
6	2.93	0.1401
7	3.26	0.1897
8	3.79	0.2695
9	4.22	0.3343
10	4.78	0.4186
11	5.64	0.5482
12	6.36	0.6566
13	6.97	0.7485
14	7.56	0.8373
15	8.10	0.9186
16	8.64	1

Table A.12 : Experimental first mode shape at 273.1Hz for a beam with slot at 7cm position and 3mm depth.

Position(cm)	V.(r.m.s) mv	V.norm.
0	2.16	0
1	2.23	0.0106
2	2.30	0.0212
3	2.47	0.047
4	2.63	0.0713
5	2.81	0.0986
6	3.08	0.1396
7	3.41	0.1897
8	3.48	0.2003
9	3.70	0.2336
10	4.86	0.4097
11	5.76	0.5463
12	6.48	0.6555
13	7.08	0.7466
14	7.69	0.8392
15	8.22	0.9196
16	8.75	1

Table A.13 : Experimental first mode shape at 274.1Hz for a beam with slot at 8cm position and 3mm depth.

Position(cm)	V.(r.m.s) mv	V.norm.
0	2.10	0
1	2.17	0.0106
2	2.24	0.0212
3	2.43	0.0502
4	2.56	0.0700
5	2.76	0.1005
6	3.08	0.1492
7	3.35	0.1903
8	3.87	0.2694
9	4.30	0.3348
10	4.86	0.4201
11	5.69	0.5464
12	6.41	0.6560
13	7.01	0.7473
14	7.61	0.8386
15	8.14	0.9193
16	8.67	1

Table A.14 : Experimental first mode shape at 266.7 Hz for cracked beam at 1cm position.

Position(cm)	V.(r.m.s) mv	V.norm.
0	2.00	0
1	2.08	0.012
2	2.16	0.024
3	2.34	0.0512
4	2.49	0.0738
5	2.73	0.1099
6	2.99	0.1491
7	3.40	0.2108
8	3.79	0.2695
9	4.23	0.3358
10	4.86	0.4308
11	5.73	0.5617
12	6.37	0.6581
13	6.99	0.7515
14	7.72	0.8614
15	8.18	0.9307
16	8.64	1

Table A.14 : Experimental first mode shape at 271.3 Hz for cracked beam at 3cm position.

Position(cm)	V.(r.m.s) mv	V.norm.
0	2.10	0
1	2.17	0.0105
2	2.24	0.021
3	2.44	0.0511
4	2.58	0.0722
5	2.83	0.1097
6	3.09	0.1488
7	3.49	0.209
8	3.86	0.2646
9	4.31	0.3323
10	4.96	0.4301
11	5.82	0.5594
12	6.47	0.6571
13	7.10	0.7519
14	7.81	0.8586
15	8.28	0.9293
16	8.75	1

Table A.14 : Experimental first mode shape at 273.2 Hz for cracked beam at 5cm position.

Position(cm)	V.(r.m.s) mv	V.norm.
0	2.00	0
1	2.08	0.012
2	2.16	0.024
3	2.34	0.0513
4	2.48	0.0724
5	2.73	0.1101
6	3.99	0.1493
7	3.39	0.2096
8	3.76	0.2655
9	4.25	0.3394
10	4.88	0.4344
11	5.71	0.5595
12	6.36	0.6576
13	6.99	0.7526
14	7.73	0.8642
15	8.18	0.9321
16	8.63	1

Table A.14 : Experimental first mode shape at 272.8 Hz for cracked beam at 6cm position.

Position(cm)	V.(r.m.s) mv	V.norm.
0	1.95	0
1	2.04	0.0136
2	2.13	0.0273
3	2.31	0.0545
4	2.44	0.0742
5	2.68	0.1106
6	2.94	0.15
7	3.34	0.2106
8	3.71	0.2666
9	4.19	0.3394
10	5.32	0.5106
11	5.65	0.5606
12	6.31	0.6606
13	6.98	0.7621
14	7.67	0.8666
15	8.11	0.9333
16	8.55	1

Appendix B

APPENDIX B

PROGRAM I

```
C     ********************************************
C     *                                          *
C     *              PROGRAM I                   *
C     *                                          *
C     ********************************************

      THIS PROGRAM IS USED TO GET THE VALUE OF THE
       SPRING CONSTANT K (XK) AT THE CLAMPED END IN
      N.M/RAD.
      THE VALUE OF FREQUENCY F SHOWLD BE GIVEN TO
      THIS PROGRAM IN Hz.
      ------------------------------------------

      REAL B2, B3
      DO 10 F=100., 315.,5.

      OPEN(UNIT=6,FILE='PROGRAM1.OUT',STATUS='NEW')
C     WRITE(*,*)'F (Hz)'
       READ(5,*)F
      W=F*2.*3.14
      R=0.78196
      EL=0.16
      E=200.E9
      SI=((0.0099**4)/12.)
      EI=E*SI
      B=((R*(W**2))/EI)**.25
      SER=B*EL
      A1=(COSH(SER)+COS(SER))/(2.*EI*B)
      A2=(SINH(SER)-SIN(SER))/(2.*EI*B)
      A3=(COSH(SER)+COS(SER))/(2.*EI*B)
      A4=(SINH(SER)-SIN(SER))/(2.*EI*B)
      B2=A1*(COSH(SER))-A2*(SIN(SER))+A3*(COS(SER))
     &-A4*(SINH(SER))
      B3=-SIN(SER)*COSH(SER)+(SINH(SER))*(COS(SER))
      XK=-B3/B2
      FF=F/313.13
50    WRITE(6,*)FF,XK
10       CONTINUE
70    STOP
      END
```

```
      IMPLICIT DOUBLE PRECISION (A-H,O-Z)
C     ********************************************
C     *                                          *
C     *            PROGRAM II                    *
C     *                                          *
C     ********************************************
C     THIS PROGRAM IS USED TO EVALUATE THE VALUE OF
C     THE FREQUENCY AT ANY MODE FOR CRACKED
C     AND UNCRACKED BEAM UTILIZING BISECTION  METHOD
C     THE VALUE OF THE CRACK LOCATION (EL1) SHOULD
C     BE GIVEN IN m BUT THE CRACK DEPTH (A1) SHOULD
C     BE GIVEN IN mm. THE OBTAINED VALUE IS LAMBDA
C     SO THE INITIAL CONDITION A, B SHOULD BE GIVEN
C     ACCORDING TO LAMBDA RANGE FOR EACH MODE SHAPE
C     ************************************************
      OPEN(UNIT=6,FILE='PROGRAM2.OUT',STATUS='NEW')
      READ(5,*)A,B
      RO=.78196
      EI=200.E9*(9.9E-3)**4./12.
       A=16.
      B=20.
      N=100
      EPS=.00001
      WRITE(6,*)'        I','    X','         F(X)'


      FA=F(A)
      FB=F(B)

      IF(FA*FB.GT.0) GOTO 111
      IF(FA.EQ.0) GOTO 11
      IF(FB.EQ.0) GOTO 22

      I=1
 1    X=(A+B)/2.0
      e=ABS((B-A)/(A+B))
      FX=F(X)
      WRITE(6,*)I,X,FX
      IF(ABS(FX).LE.EPS) GOTO 222
      I=I+1
      IF (I.GT.N)STOP
      IF(FA*FX)2,3,4
 2    B=X
      FB=FX
      GOTO 1
 4    A=X
      FA=FX
      GOTO 1
 3    WRITE(6,*)X

      GOTO 222
 11   WRITE(*,*)'THE ROOT IS',A ,'F(X)=',F(A)
      GOTO 222
 22   WRITE(*,*)'THE ROOT IS',B, 'F(X)=',F(B)
      GOTO 222
 111  WRITE(*,*)'EACH OF THEM HAVE THE SAME SIGN'
      STOP


 222  NAT=SQRT(((X**4.)*EI)/RO)
```

```
      FREQ=NAT/(2.*3.14286)
      WRITE(6,*)X
      WRITE(6,*)'FREQ=',FREQ


      STOP
      END
C*************************************************
      FUNCTION F(X)

      EL1=.05
      A1=7.6683
      EL=0.16
      E=200.E9

      RK=13775.93

      H1=9.9
      G=A1/H1
      EI=200.E9*(9.9E-3)**4./12.
      CF=1.8624*G*G-3.95*G**3.+16.375*G**4.-37.226*G**5.
     &  +76.81*G**6.
     &  -126.9*G**7.+172.*G**8.-143.97*G**9.+66.56*G**10.
      RKR=1.0/(5.346*H1*1.E-3*CF/EI)
       WRITE(6,*)'RKR=',RKR
      P1=SINH(X*EL)*COS(X*EL)-COSH(X*EL)*SIN(X*EL)
      P2=COSH(X*EL)*COS(X*EL)-SINH(X*EL)*SIN(X*EL)
      P3=P1*(SIN(X*EL)/COS(X*EL))+COSH(X*EL)/COS(X*EL)
      P4=P2*(SIN(X*EL)/COS(X*EL))+SINH(X*EL)/COS(X*EL)
      PZ1=(SIN(X*EL1)+(RK/(2.*EI*X))*(COSH(X*EL1)
     &  -COS(X*EL1)))
     &  /(P2*COS(X*EL1)+P4*SIN(X*EL1)+COSH(X*EL1))
      PZ2=(SINH(X*EL1)+(RK/(2.*EI*X))*(COSH(X*EL1)
     &  -COS(X*EL1)))
     &   /(P2*COS(X*EL1)+P4*SIN(X*EL1)+COSH(X*EL1))
      PZ3=-(P1*COS(X*EL1)+P3*SIN(X*EL1)+SINH(X*EL1))
     &   /(P2*COS(X*EL1)+P4*SIN(X*EL1)+COSH(X*EL1))
      PZ4=(COS(X*EL1)+(RK/(2.*EI*X))*(SINH(X*EL1)
     &  +SIN(X*EL1)))
     &   /(-P2*SIN(X*EL1)+P4*COS(X*EL1)+SINH(X*EL1))
      PZ5=(((X*EI)/RKR)*(-SIN(X*EL1)+(RK/(2.*EI*X))
     &  *(COSH(X*EL1)
     &   +COS(X*EL1))))/(-P2*SIN(X*EL1)+P4*COS(X*EL1)
     &  +SINH(X*EL1))
      PZ6=(COSH(X*EL1)+(RK/(2.*EI*X))*(SINH(X*EL1)
     &  +SIN(X*EL1)))
     &   /(-P2*SIN(X*EL1)+P4*COS(X*EL1)+SINH(X*EL1))
      PZ7=(((X*EI)/RKR)*(SINH(X*EL1)+(RK/(2.*EI*X))
     &  *(COSH(X*EL1)
     &   +COS(X*EL1))))/(-P2*SIN(X*EL1)+P4*COS(X*EL1)
     &  +SINH(X*EL1))
      PZ8=-(-P1*SIN(X*EL1)+P3*COS(X*EL1)+COSH(X*EL1))
     &   /(-P2*SIN(X*EL1)+P4*COS(X*EL1)+SINH(X*EL1))
      P5=(PZ1-PZ4-PZ5)/(PZ8-PZ3)
      P6=(PZ2-PZ6-PZ7)/(PZ8-PZ3)

      PS1=(SIN(X*EL1)+(RK/(2.*EI*X))*(COSH(X*EL1)
     &  -COS(X*EL1)))
     &  /(P2*COS(X*EL1)+P4*SIN(X*EL1)+COSH(X*EL1))
      PS2=-((P1*COS(X*EL1)+P3*SIN(X*EL1)+SINH(X*EL1))*P5)
```

```
     &   /(P2*COS(X*EL1)+P4*SIN(X*EL1)+COSH(X*EL1))
         PS3=(SINH(X*EL1)+(RK/(2.*EI*X))*(COSH(X*EL1)
     &   -COS(X*EL1)))
     &   /(P2*COS(X*EL1)+P4*SIN(X*EL1)+COSH(X*EL1))
         PS4=-((P1*COS(X*EL1)+P3*SIN(X*EL1)+SINH(X*EL1))*P6)
     &   /(P2*COS(X*EL1)+P4*SIN(X*EL1)+COSH(X*EL1))
         P7=PS1+PS2
         P8=PS3+PS4



         P9=-SIN(X*EL1)+(RK/((2.*EI*X)))*(COSH(X*EL1)
     &   +COS(X*EL1))
     &   -P5*(-P1*COS(X*EL1)-P3*SIN(X*EL1)+SINH(X*EL1))
     &   -P7*(-P2*COS(X*EL1)-P4*SIN(X*EL1)+COSH(X*EL1))

         P10=SINH(X*EL1)+(RK/(2.*EI*X))*(COSH(X*EL1)
     &   +COS(X*EL1))
     &   -P6*(-P1*COS(X*EL1)-P3*SIN(X*EL1)+SINH(X*EL1))
     &   -P8*(-P2*COS(X*EL1)-P4*SIN(X*EL1)+COSH(X*EL1))

         P11=-COS(X*EL1)+(RK/(2.*EI*X))*(SINH(X*EL1)
     &   -SIN(X*EL1))
     &   -P5*(P1*SIN(X*EL1)-P3*COS(X*EL1)+COSH(X*EL1))
     &   -P7*(P2*SIN(X*EL1)-P4*COS(X*EL1)+SINH(X*EL1))

         P12=COSH(X*EL1)+(RK/(2.*EI*X))*(SINH(X*EL1)
     &   -SIN(X*EL1))
     &   -P6*(P1*SIN(X*EL1)-P3*COS(X*EL1)+COSH(X*EL1))
     &   -P8*(P2*SIN(X*EL1)-P4*COS(X*EL1)+SINH(X*EL1))

         F=P9*P12-P10*P11

         RETURN
         END
C*******************************************************
```

```
      ********************************************
      *                                          *
      *                PROGRAM III               *
      *                                          *
      ********************************************

      THIS PROGRAM IS USED TO MODE SHAPES
      THE CRACK LOCATION (EL1)IN m, CRACK DEPTH
      (A1) IN mm, AND LAMBDA (ff)SHOULD BE GIVEN
       TO THIS PROGRAM. THE VALUE OF CON. IS THE
       CONSTANT  WHIH IS USED TO NORMALIZED
      THE MODE SHAPE. at the begining con.=1
       CON.=THE MAX. AMPLITUDE

      OPEN(UNIT=6,FILE='PROGRAM3.OUT',STATUS='NEW')
      EL1=.05
      EL=0.16
      E=200.E9


      RK=13775.93

      H1=9.9
      write(*,*)'a1','ff','con'
      read(5,*)a1,ff,con
      SS=A1/H1
      EI=(200.E9*(9.9E-3)**4.)/12.
      CF=1.8624*SS*SS-3.95*SS**3.+16.375*SS**4.
     &  -37.226*SS**5.+76.81*SS**6.
     &  -126.9*SS**7.+172.*SS**8.-143.97*SS**9.+66.56*SS**10.
      RKR=1.0/((5.346*H1*1.E-3*CF)/EI)



      P1=SINH(FF*EL)*COS(FF*EL)-COSH(FF*EL)*SIN(FF*EL)
      P2=COSH(FF*EL)*COS(FF*EL)-SINH(FF*EL)*SIN(FF*EL)
      P3=P1*(SIN(FF*EL)/COS(FF*EL))+COSH(FF*EL)/COS(FF*EL)
      P4=P2*(SIN(FF*EL)/COS(FF*EL))+SINH(FF*EL)/COS(FF*EL)
      PZ1=(SIN(FF*EL1)+(RK/(2.*EI*FF))*(COSH(FF*EL1)-COS(FF*EL1)))
     &  /(P2*COS(FF*EL1)+P4*SIN(FF*EL1)+COSH(FF*EL1))
      PZ2=(SINH(FF*EL1)+(RK/(2.*EI*FF))*(COSH(FF*EL1)-COS(FF*EL1)))
     &   /(P2*COS(FF*EL1)+P4*SIN(FF*EL1)+COSH(FF*EL1))
      PZ3=-(P1*COS(FF*EL1)+P3*SIN(FF*EL1)+SINH(FF*EL1))
     &   /(P2*COS(FF*EL1)+P4*SIN(FF*EL1)+COSH(FF*EL1))
      PZ4=(COS(FF*EL1)+(RK/(2.*EI*FF))*(SINH(FF*EL1)+SIN(FF*EL1)))
     &   /(-P2*SIN(FF*EL1)+P4*COS(FF*EL1)+SINH(FF*EL1))
      PZ5=(((FF*EI)/RKR)*(-SIN(FF*EL1)+(RK/(2.*EI*FF))*(COSH(FF*EL1)
     &   +COS(FF*EL1))))/(-P2*SIN(FF*EL1)+P4*COS(FF*EL1)+SINH(FF*EL1))
      PZ6=(COSH(FF*EL1)+(RK/(2.*EI*FF))*(SINH(FF*EL1)+SIN(FF*EL1)))
     &   /(-P2*SIN(FF*EL1)+P4*COS(FF*EL1)+SINH(FF*EL1))
      PZ7=(((FF*EI)/RKR)*(SINH(FF*EL1)+(RK/(2.*EI*FF))*(COSH(FF*EL1)
     &   +COS(FF*EL1))))/(-P2*SIN(FF*EL1)+P4*COS(FF*EL1)+SINH(FF*EL1))
      PZ8=-(-P1*SIN(FF*EL1)+P3*COS(FF*EL1)+COSH(FF*EL1))
     &   /(-P2*SIN(FF*EL1)+P4*COS(FF*EL1)+SINH(FF*EL1))
      P5=(PZ1-PZ4-PZ5)/(PZ8-PZ3)
      P6=(PZ2-PZ6-PZ7)/(PZ8-PZ3)

      PS1=(SIN(FF*EL1)+(RK/(2.*EI*FF))*(COSH(FF*EL1)-COS(FF*EL1)))
     &  /(P2*COS(FF*EL1)+P4*SIN(FF*EL1)+COSH(FF*EL1))
```

```
      PS2=-((P1*COS(FF*EL1)+P3*SIN(FF*EL1)+SINH(FF*EL1))*P5)
     &  /(P2*COS(FF*EL1)+P4*SIN(FF*EL1)+COSH(FF*EL1))
      PS3=(SINH(FF*EL1)+(RK/(2.*EI*FF))*(COSH(FF*EL1)-COS(FF*EL1)))
     &  /(P2*COS(FF*EL1)+P4*SIN(FF*EL1)+COSH(FF*EL1))
      PS4=-((P1*COS(FF*EL1)+P3*SIN(FF*EL1)+SINH(FF*EL1))*P6)
     &  /(P2*COS(FF*EL1)+P4*SIN(FF*EL1)+COSH(FF*EL1))
      P7=PS1+PS2
      P8=PS3+PS4


      P9=-SIN(FF*EL1)+(RK/((2.*EI*FF)))*(COSH(FF*EL1)+COS(FF*EL1))
     &  -P5*(-P1*COS(FF*EL1)-P3*SIN(FF*EL1)+SINH(FF*EL1))
     &  -P7*(-P2*COS(FF*EL1)-P4*SIN(FF*EL1)+COSH(FF*EL1))

      P10=SINH(FF*EL1)+(RK/(2.*EI*FF))*(COSH(FF*EL1)+COS(FF*EL1))
     &  -P6*(-P1*COS(FF*EL1)-P3*SIN(FF*EL1)+SINH(FF*EL1))
     &  -P8*(-P2*COS(FF*EL1)-P4*SIN(FF*EL1)+COSH(FF*EL1))

      P11=-COS(FF*EL1)+(RK/(2.*EI*FF))*(SINH(FF*EL1)-SIN(FF*EL1))
     &  -P5*(P1*SIN(FF*EL1)-P3*COS(FF*EL1)+COSH(FF*EL1))
     &  -P7*(P2*SIN(FF*EL1)-P4*COS(FF*EL1)+SINH(FF*EL1))

      P12=COSH(FF*EL1)+(RK/(2.*EI*FF))*(SINH(FF*EL1)-SIN(FF*EL1))
     &  -P6*(P1*SIN(FF*EL1)-P3*COS(FF*EL1)+COSH(FF*EL1))
     &  -P8*(P2*SIN(FF*EL1)-P4*COS(FF*EL1)+SINH(FF*EL1))


      DO 12 X=.0,EL1,.001
      F=-(P10/P9)*(SIN(FF*X)+(RK/(2.*EI*FF))*(COSH(FF*X)-COS(FF*X)))
     &  +SINH(FF*X)+(RK/(2.*EI*FF))*(COSH(FF*X)-COS(FF*X))

      F=F/con
      XS=X/EL
12    WRITE(6,*)XS,F
      X=EL1
      F=-(P10/P9)*(SIN(FF*X)+(RK/(2.*EI*FF))*(COSH(FF*X)-COS(FF*X)))
     &  +SINH(FF*X)+(RK/(2.*EI*FF))*(COSH(FF*X)-COS(FF*X))

      F=F/con
      XS=X/EL
        WRITE(6,*)XS,F
      G=-(P10/P9)*(P5*(P1*COS(X*FF)+P3*SIN(FF*X)
     &  +SINH(FF*X))+P7*(P2*COS(FF*X)+P4*SIN(X*FF)
     &  +COSH(FF*X)))
     &  +(P6*(P1*COS(X*FF)+P3*SIN(FF*X)
     &  +SINH(FF*X))+P8*(P2*COS(FF*X)+P4*SIN(X*FF)
     &  +COSH(FF*X)))
        WRITE(6,*)
      G=G/con
      XS=X/EL
        WRITE(6,*)XS,G
      DO 11 X=EL1,EL,.001
      G=-(P10/P9)*(P5*(P1*COS(X*FF)+P3*SIN(FF*X)
     &  +SINH(FF*X))+P7*(P2*COS(FF*X)+P4*SIN(X*FF)
     &  +COSH(FF*X)))
     &  +(P6*(P1*COS(X*FF)+P3*SIN(FF*X)
     &  +SINH(FF*X))+P8*(P2*COS(FF*X)+P4*SIN(X*FF)
     &  +COSH(FF*X)))
      G=G/con
```

```
      ****************************************
      *                                      *
      *            PROGRAM IV                *
      *                                      *
      ****************************************

      THIS PROGRAM IS USED TO GET THE VALUES OF
      THE SLOPE. THE CRACK LOCATION( EL1) SHOULD
      BE GIVEN IN m. THE CRACK DEPTH (A1) SHOULD
      BE GIVEN IN mm. THE VALUE OF CON. THE
      CONSTANT OF NORMALIZATION=1, AFTER THAT
      CON.= THE MAX. VALUE OF THE SLOPE
      THE VALUE OF LAMBDA (FF) SHOULD BE GIVEN


      OPEN(UNIT=6,FILE='PROGRAM4.OUT',STATUS='NEW')
      EL1=.02
      EL=0.16
      E=200.E9

      READ(5,*)A1, FF, CON
      RK=13775.93

      H1=9.9

      SS=A1/H1
      EI=(200.E9*(9.9E-3)**4.)/12.
      CF=1.8624*SS*SS-3.95*SS**3.+16.375*SS**4.
     &  -37.226*SS**5.+76.81*SS**6.
     &  -126.9*SS**7.+172.*SS**8.-143.97*SS**9.
     &  +66.56*SS**10.
      RKR=1.0/((5.346*H1*1.E-3*CF)/EI)


      P1=SINH(FF*EL)*COS(FF*EL)-COSH(FF*EL)*SIN(FF*EL)
      P2=COSH(FF*EL)*COS(FF*EL)-SINH(FF*EL)*SIN(FF*EL)
      P3=P1*(SIN(FF*EL)/COS(FF*EL))+COSH(FF*EL)/COS(FF*EL)
      P4=P2*(SIN(FF*EL)/COS(FF*EL))+SINH(FF*EL)/COS(FF*EL)
      PZ1=(SIN(FF*EL1)+(RK/(2.*EI*FF))*(COSH(FF*EL1)
     &  -COS(FF*EL1)))
     &  /(P2*COS(FF*EL1)+P4*SIN(FF*EL1)+COSH(FF*EL1))
      PZ2=(SINH(FF*EL1)+(RK/(2.*EI*FF))*(COSH(FF*EL1)
     &  -COS(FF*EL1)))
     &   /(P2*COS(FF*EL1)+P4*SIN(FF*EL1)+COSH(FF*EL1))
      PZ3=-(P1*COS(FF*EL1)+P3*SIN(FF*EL1)+SINH(FF*EL1))
     &   /(P2*COS(FF*EL1)+P4*SIN(FF*EL1)+COSH(FF*EL1))
      PZ4=(COS(FF*EL1)+(RK/(2.*EI*FF))*(SINH(FF*EL1)
     &   +SIN(FF*EL1)))
     &   /(-P2*SIN(FF*EL1)+P4*COS(FF*EL1)+SINH(FF*EL1))
      PZ5=(((FF*EI)/RKR)*(-SIN(FF*EL1)+(RK/(2.*EI*FF))
     &  *(COSH(FF*EL1)
     &   +COS(FF*EL1))))/(-P2*SIN(FF*EL1)+P4*COS(FF*EL1)
     &  +SINH(FF*EL1))
      PZ6=(COSH(FF*EL1)+(RK/(2.*EI*FF))*(SINH(FF*EL1)
     &  +SIN(FF*EL1)))
     &   /(-P2*SIN(FF*EL1)+P4*COS(FF*EL1)+SINH(FF*EL1))
      PZ7=(((FF*EI)/RKR)*(SINH(FF*EL1)+(RK/(2.*EI*FF))
     &  *(COSH(FF*EL1)
     &   +COS(FF*EL1))))/(-P2*SIN(FF*EL1)+P4*COS(FF*EL1)
```

```
     &   +COSH(FF*X))+P8*(-P2*SIN(FF*X)+P4*COS(X*FF)
     &   +SINH(FF*X))))
           WRITE(6,*)
         G=-G/CON

           WRITE(6,*)X,G
         DO 11 X=EL1,EL,.001
         G=FF*(-(P10/P9)*(P5*(-P1*SIN(X*FF)+P3*COS(FF*X)
     &   +COSH(FF*X))+P7*(-P2*SIN(FF*X)+P4*COS(X*FF)
     &   +SINH(FF*X)))
     &   +(P6*(-P1*SIN(X*FF)+P3*COS(FF*X)
     &   +COSH(FF*X))+P8*(-P2*SIN(FF*X)+P4*COS(X*FF)
     &   +SINH(FF*X))))
         G=-G/CON

11       WRITE(6,*)X,G

       STOP
        END
```

```
C*****************************************************
C*                                                   *
C*                   PROGRAM V                       *
C*                                                   *
C*****************************************************

      THIS PROGRAM IS USED TO EVALUATE THE COMPLIANCE
      AND THE SPRING CONSTANT VALUE AT THE CRACK LOCA
      TION ACCORDING TO DIMAROGONAS CORELATION. THE
      VALUE OF THE CRACK SHOULD BE GIVEN (A1) TO THE
      PROGRAM

      OPEN(UNIT=6,FILE='PROGRAM5.OUT',STATUS='NEW')
      DO 10 A1=.000001,9.9,.1
      EL1=.03
      EL=0.16
      E=200.E9

      RK=13775.93

      H1=9.9
      G=A1/H1
      EI=200.E9*(9.9E-3)**4./12.
      CF=1.8624*G*G-3.95*G**3.+16.375*G**4.-37.226*G**5.
     &  +76.81*G**6.
     &  -126.9*G**7.+172.*G**8.-143.97*G**9.+66.56*G**10.
      C=(5.346*H1*1.E-3*CF/EI)
      RKR=1.0/C
10      WRITE(6,*)A1,RKR

      STOP
      END
```

الملخـــــص

تهدف هذه الرسالة إلى دراسة الأثر الذي تحدثه التشققات – المتواجدة في (الجيزان الكوبولية) – على السلوك (الديناميكي) لهذه (الجيزان) في كل من المجالين النظري والعلمي. ومن الجدير ذكره أن التغير الذي يحصل على (الطور الأول للجيزان الكوبولية) هو الأساس الذي قامت عليه هذه الدراسة. وقد تم التوصل إلى أنه ومن خلال الأثر الذي تحدثه التشققات على سلوك (الجيزان الكوبولية) فإنه يمكن تحديد مكان الشق وعمقه.

لقد تم في هذا البحث التطرق إلى إحدى الطرق التي وضعت لتحديد الشقوق, حيث تم الكشف على عدة عيوب في تلك الطريقة. ولذلك فإن طريقة جديدة للبحث عن الشقوق, يتوقع بأن تكون أكثر شمولية من الطريقة االسابقة تم بحثها في هذه الرسالة. هنالك مجموعة من البرامج وضعت خصيصاً لحل المعادلات الرياضية التي تم التوصل إليها للحصول على النتائج المطلوبة التي تستخدم في تحديد الشقوق.. وفي النهاية تم التطرق إلى مجموعة من الإستنتاجات والتوصيات لفتح آفاق جديدة في مجال البحث عن الشقوق بواسطة طرق الإهتزازات الميكانيكية.